



HAL
open science

Adsorption of hexavalent chromium by activated carbon obtained from a waste lignocellulosic material (*Ziziphus jujuba* cores): Kinetic, equilibrium, and thermodynamic study

Radia Labied, Oumessaad Benturki, Adh' Ya Eddine Hamitouche, André Donnot

► To cite this version:

Radia Labied, Oumessaad Benturki, Adh' Ya Eddine Hamitouche, André Donnot. Adsorption of hexavalent chromium by activated carbon obtained from a waste lignocellulosic material (*Ziziphus jujuba* cores): Kinetic, equilibrium, and thermodynamic study. *Adsorption Science and Technology*, 2017, 36 (3-4), pp.1066-1099. 10.1177/0263617417750739 . hal-02982841

HAL Id: hal-02982841

<https://hal.univ-lorraine.fr/hal-02982841>

Submitted on 3 Jun 2021

HAL is a multi-disciplinary open access archive for the deposit and dissemination of scientific research documents, whether they are published or not. The documents may come from teaching and research institutions in France or abroad, or from public or private research centers.

L'archive ouverte pluridisciplinaire **HAL**, est destinée au dépôt et à la diffusion de documents scientifiques de niveau recherche, publiés ou non, émanant des établissements d'enseignement et de recherche français ou étrangers, des laboratoires publics ou privés.



Distributed under a Creative Commons Attribution 4.0 International License

Adsorption of hexavalent chromium by activated carbon obtained from a waste lignocellulosic material (*Ziziphus jujuba* cores): Kinetic, equilibrium, and thermodynamic study

Adsorption Science & Technology
2018, Vol. 36(3–4) 1066–1099
© The Author(s) 2018
DOI: 10.1177/0263617417750739
journals.sagepub.com/home/adt



Radia Labied

USTHB, Algeria; Centre de Recherche Scientifique et Technique en Analyses Physico-chimiques (C.R.A.P.C), Algeria

Oumessaad Benturki

USTHB, Algeria

Adh' Ya Eddine Hamitouche

Centre de Recherche Scientifique et technique en analyses physico chimiques (C.R.A.P.C)

André Donnot

Université, Henri Poincaré—Nancy I, France

Abstract

In aqueous solutions, hexavalent chromium Cr(VI) was successfully removed by activated carbon “*Z. jujuba* rubidium carbonate-activated carbon” obtained from waste lignocellulosic material (*Ziziphus jujuba* cores). Rubidium carbonate was used to prepare *Z. jujuba* rubidium carbonate-activated carbon by chemical activation using a 1:1 w/w ratio. Our results indicate that the obtained surface area of the activated carbon was equal to 608.31 m²/g. The adsorption study of Cr(VI) was investigated under batch conditions at constant stirring speed (220 r/min). Factors such as pH (1–6), temperature (20–40°C), adsorbent concentration (0.5–3 g/l), and initial Cr(VI)

Corresponding author:

Radia Labied, Department of Biology, Laboratory of Ecology and Environment, USTHB, Algiers 16000, Algeria.
Email: labiedr@yahoo.fr



Creative Commons CC-BY: This article is distributed under the terms of the Creative Commons Attribution 4.0 License (<http://www.creativecommons.org/licenses/by/4.0/>) which permits any use,

reproduction and distribution of the work without further permission provided the original work is attributed as specified on the SAGE and Open Access pages (<https://us.sagepub.com/en-us/nam/open-access-at-sage>).

concentration (50–500 mg/l) were all studied to attain the maximum removal efficiency. Prior to the adsorption process, the morphology, elementary composition, and loss mass of activated carbon were characterized using scanning electron microscopy, X-ray fluorescence spectrometry, Fourier transform infrared spectroscopy, and thermogravimetric analysis. Fourier transform infrared analysis of the adsorbent demonstrated the presence of key functional groups associated with the adsorption phenomenon such as those of hydroxyl and aromatic groups. The obtained results showed that the optimal conditions for a maximum adsorption efficiency are 2 for pH, 1 g/l for activated carbon dosage and 100 mg/l for Cr(VI) concentration. The removal percentage increased from 27.2 to 62.08%. The kinetic sorption was described by a pseudo-second-order kinetic equation ($R^2 \approx 0.995$). The Tóth ($R^2 = 0.997$) and Elovich models were best to explain the sorption phenomenon. Thermodynamic studies showed that the adsorption of Cr(VI) onto activated carbon was feasible, spontaneous, and endothermic at 20–40°C. This novel *Z. jujuba* rubidium carbonate-activated carbon derived from *Z. jujuba* core has been found to be effective for the removal of Cr(VI) and not harmful to the ecosystem.

Keywords

Ziziphus jujuba, chromium, activated carbon, adsorption, removal, isotherm

Submission date: 11 July 2017; Acceptance date: 16 November 2017

Introduction

The rapid industrialization and urbanization of our cities have resulted in the discharge of high levels of toxic heavy metals such as chromium, lead, mercury, cadmium, and cobalt into the mainstreams of our wastewater systems. These metals tend to possess greater stability and can cause a detrimental impact on our ecosystem as well as our public health once disposed untreated into our environment (Ciopec et al., 2012; Wang and Chen, 2006).

Chromium (Cr) is one of the most naturally abundant water contaminants. The latter exists in a series of oxidation states from -2 to $+6$ valence electrons; the most important stable states are 0 (element metal), $+3$ (trivalent), and $+6$ (hexavalent). Cr^{3+} and Cr^{6+} are released into the environment from stationary point sources resulting from human activities. The metal can cause acute and chronic adverse effects in warm-blooded organisms. Most investigators agree that chromium probably exists in biological species in its trivalent state; the main human exposure of Cr(III) comes from diet (Khezami and Capart, 2005; Nabi et al., 2011).

Hexavalent chromium is present in the effluents produced from electroplating, leather tanning, cement, mining, dyeing, fertilizer, and photography industries and can result in severe environmental and public health problems (Demirbas et al., 2004). In general, Cr(VI) concentrations in industrial wastewater range from 0.5 to 270 mg/l; effluents from tannery factories can contain 1300–2500 mg/l of Cr(VI) (Liu et al., 2006) while its tolerance limit in surface wastewater as current recommended by USEPA and the European Union is below 0.05 mg/l. The total concentration of chromium, including Cr(III), Cr(VI) and other forms is usually regulated to values below 2 mg/l (Baral and Engelken, 2002; Park et al., 2008).

There exists many methods in literature which can remove metal ion pollutants from aqueous solutions, and such approaches can be in the form of physical, chemical, and/or

biological techniques (Sahinkaya et al., 2012). The traditional physicochemical methods used for (Cr) removal including, but are not limited to chemical precipitation (Monser and Adhoum, 2002), oxidation or reduction (Sedlak and Chan, 1997), ion exchange (Yang et al., 2014), electrochemical treatment (Giri et al., 2012), membrane technology (Hafez et al., 2002), evaporation recovery (Tiravanti et al., 1997), and adsorption onto activated carbon (Deveci and Kar, 2013; Suksabye and Thiravetyan, 2012). Adsorption plays an important role in the improvement of water quality; generally, activated carbon can be used to adsorb metals. The utilization of adsorption methods in this area of research has attracted the attention of many scientists from around the world; however, the process cannot pay much attention but can be both technically and economically challenging in terms of time and costs associated with developing a custom-made methodology for each unique contaminated aqueous solution. The high specific surface area, the microporous character, and the surface chemical nature of activated carbons made them suitable for examination as potential adsorbents for the removal of heavy metals from industrial wastewater (Dobrowolski and Stefaniak, 2000; Kadirvelu and Namasivayam, 2003). In spite of their advantages, they also show many shortcomings such as high preparation cost, reactivation resulting from adsorption saturation, and selectivity challenges. Recently, much attention has been drawn from scientists toward the utilization of biomaterials, which are by-products or wastes derived from large-scale agricultural operations, for the removal of Cr(VI) via synthesis of activated carbon. Among these, less expensive, nonconventional adsorbents, such as apple waste, peanut hull carbon, agricultural wastes, rice husk and straw (Bishnoi et al., 2004; Hsu et al., 2009); hazelnut shell, coconut shell (Babel and Kurniawan, 2004); cornelian cherry, apricot stone, almond shells (Demirbas et al., 2004); *Casuarina equisetifolia* leaves (Ranganathan, 2000); tamarind wood (Acharya et al., 2009); *Hevea brasiliensis* sawdust (Karthikeyan et al., 2005); date palm seeds (Nemr et al., 2008); olive bagasse (Demiral et al., 2008); *Eichhornia crassipes* root (Duranoglu et al., 2010); *Trapa natans* husk (Gottipati and Mishra, 2010); *Terminalia arjuna* nuts (Cronje et al., 2011); peanut shells, jatropha wood (Giri et al., 2012); and longan seed (Yang et al., 2015) were all used to remove heavy metals from industrial wastewater. *Z. jujuba*, a very important fruit, is a thorny shrub Rhamnaceae fruit, found in the Mediterranean region; its abundance in nature is also important, especially in our country, where it is usually consumed in large quantities. Jujube cores are considered as an agricultural waste and an animal feedstock. The samples were collected from “Medea,” a town situated 80 km south west of Algiers (Algeria); in order for them to be valorized in different areas of chemical processes, this valorization has been widely shared by other team members, (Bouras et al., 2015) especially in the field of wastewater treatment. As a result, it is considered as an excellent precursor for the synthesis of an activated carbon due to its natural abundance; for this reason, many researchers in our laboratory have worked on jujube cores to remove phenols (P), para-cresol, 2,4-dichlorophenol, 4-amino phenol, pesticides, humic acid, textile dyes, and hexavalent chromium from aqueous solutions.

The aim of this research work is to valorize *Z. jujuba* cores, a naturally abundant vegetable waste material, in the area of wastewater treatment; the process involves initial conversion of the material into activated carbon using a novel rubidium carbonate procedure. The resulting product is then used to study its efficiency to remove hexavalent chromium Cr(VI) from aqueous solutions in a batch operating mode; in this work, we also evaluate the effect of various factors on Cr(VI) removal. However, to the best of our knowledge, no investigation has been done in this way; moreover, the modeling of hexavalent

chromium adsorption data by various models (kinetic and isotherms) is carried out using a nonlinear regression analysis. Additionally, the effects of some associated operating conditions such as the adsorbent dose as a function of temperature were not previously studied.

Experimental

Chemicals

In all experiments, distilled water was used for preparation. Potassium dichromate ($K_2Cr_2O_7$), hydrochloric acid (HCl), sodium hydroxide (NaOH), and rubidium carbonate (Rb_2CO_3) were purchased from Sigma Aldrich. A stock solution containing chromium 1 g/l was prepared by dissolving 2.829 g of potassium dichromate in 1000 ml of bidistilled water. The desired concentrations were obtained by diluting the stock solution with distilled water to obtain concentrations ranging from 50 to 500 mg/l.

Preparation of activated carbon

Z. jujuba fruit and cores were collected from "Medea" (Algeria); jujube cores were washed with distilled water and dried in a steam room at 110°C over the course of 24 h. After cooling, the cores were crushed and sieved by AFNOR-type sieve, the grading size of cores obtained was between 500 and 1000 µm, the cores were dried again at 110°C over a period of 24 h; these cores were activated chemically by solid rubidium carbonate using a 1:1 w/w ratio; after mixing, the product was placed on a nacelle for carbonization; nitrogen was circulated through the system for 30 min to purge air from the system. The mixture was heated at 800°C with a rate of 5°C/min and kept at this temperature for 1 h; the carbonized sample was abbreviated as ZRC-AC (*Z. jujuba* rubidium carbonate-activated carbon). After cooling under nitrogen flow, the activated product was subsequently removed from the furnace and refluxed with 10 ml of HCl (0.1 N) for 3 h to remove inorganic impurities. The remaining solid was followed by rinsing again with distilled water until the pH of the washing solution was in the range of 5.5–6.0. After that, the activated carbon was dried overnight in an oven at 110°C, crushed and sieved between 500 and 1000 µm; finally, the granular carbon was kept in a desiccator under vacuum until further use.

Charaterization of solid adsorbent

Global chemical analysis. Measurement of the ash rate: The ash is the criterion used for the determination of contaminants of inorganic products in the starting material. The ash content is determined using the following procedure: A sample weighting between 1 and 2 g and sieved between 0.15 and 0.25 mm was dried in an oven for 12 h and then placed in a porcelain dish. This capsule was introduced into a horizontal oven open to air and then heated for an initial half hour at 773 K allowed by 4 h at 1085 K. Once the incineration was completed, the furnace was allowed to cool to room temperature and the capsule was weighed.

The chemical composition of the biomass *Z. jujuba* cores has been done using Thermofinnigan Flash EA, 1112 apparatus (Benturki, 2008).

X-ray fluorescence (XRF) spectrometry analysis: XRF analysis was used to analyze oxides in both the biomass and activated carbon.

BET surface area and pore distribution. To identify the porous texture of our activated carbon, N_2 adsorption–desorption technique was sought using Micrometrics apparatus (ASAP 2010) at -196°C . The surface area of our activated carbon was calculated using Brunauer–Emmett–Teller (BET) equation within the pressure range 0.05–0.35. The micro-pore volume, area, and external surface area were determined using t-plot method. The total pore volume, calculated from a liquid volume of adsorbate adsorbed at a relative pressure of $p/p_0 = 0.989$, as well as the median pore diameter was obtained using Horvath–Kawazoe method. The mesopore volume was calculated by subtracting the micropores volume from the total pore volume (Gregg and Sing, 1982).

Scanning electron microscopy (SEM). The particle size and morphological feature of activated carbon before and after adsorption of a Cr(VI) were analyzed using SEM QUANTA 250 with an acceleration voltage of 20.00 kV and a working distance of 10.0 mm. The samples were deposited on a disk holder and protected by a carbon tape for it to be fixed; photography was performed using an Everhart–Thornley detector with high vacuum mode and/or circular back scatter detector for contrast. The surface elemental analysis of the activated carbon was carried out using energy dispersed X-ray spectroscopy. The spectra were recorded using EDAX AMATEK equipment.

Fourier transform infrared (FTIR) analysis. The surface chemical characteristics of the biomass and the activated carbon were characterized using Bruker Alpha FTIR spectrometer; the samples were prepared using the KBr pellet technique by mixing a small amount of an activated carbon with 100 mg of dried, spectroscopic grade, KBr which was previously grinded and pressed into a pellet by applying a pressure of 1200 lbf/in² for about 5 min (the concentration of the sample in KBr should be in the range of 1%); the transparent pellet was dried in an oven at 30°C overnight and then inserted into the instrument; then, the spectra were recorded over the range 4000–400 cm^{-1} with a spectral resolution of 2 cm^{-1} and a total number of 64 scans.

Ultraviolet–visible (UV–visible) spectroscopy analysis. The remaining concentration of Cr(VI) ions in solution was measured using UV–visible spectroscopy after reaction with 1,5-diphenyl-carbazide; the procedure was performed following a standard method introduced by Gilcreas et al. (1965) using Varian Cary 50 Scan UV–Visible spectrophotometer at wavelength of $\lambda = 540$ nm.

pH point of zero charge measurements “ pH_{pzc} ”. The activated carbon pH point of zero charge (pH_{pzc}) is defined as the pH of aqueous solution in which the solid exists under neutral electrical potential, and this was identified using the experimental protocol defined by Lopez-Ramon et al. (1999) on the characterization of acidic and basic surface sites on carbon using various techniques. Flasks of NaCl solutions containing 0.1 M concentration with pH values ranging from 2 to 10, normally adjusted with 0.01 M solutions of HCl or NaOH, were prepared; 0.1 g of activated carbon was mixed with 20 ml of each solution and stirred for 72 h followed by filtration; the pH of the resulting solution was then measured; finally, the curve of final pH as a function of initial pH was established. The pH_{pzc} corresponds to the pH of solution for which the lines meet at the common intersection point.

Thermogravimetric analysis (TGA). TGA consists of measuring the mass variation of a sample as a function of temperature. It was carried out on an SDT Q600 thermo balance (TA Instruments) under controlled atmosphere (nitrogen) to avoid the combustion of activated carbon. The activated carbon to be analyzed (10–15 mg) is placed in the sample crucible while an empty crucible is placed on the reference arm of the scale. The furnace begins to heat; the temperature rise can be carried out from room temperature to 1500°C at a ramp of 10°C/min.

Batch adsorption study

Kinetic study. In order to study the adsorption of Cr(VI) ions onto activated carbon and the effect of diverse parameters on the adsorption kinetic, an experimental series have been performed on a mechanical shaker equipped with a thermostatic water bath set between 180 and 200 blow per minute (bpm), using a 250 ml conical flask. A series of adsorption experiments were performed.

The first series was to investigate the effect of contact time and initial solution pH, varying from 1 to 6, by adding (0.1 N) of HCl and/or NaOH; the adsorption kinetic of Cr(VI) ions was studied at an initial Cr(VI) concentration equal to 100 mg/l, adsorbent dose of 1 g/l, temperature of 30°C, and a contact time ranging from 5 to 1440 min. The second series of experiments was to study the adsorption kinetic under the effect of temperature ranging between 20, 30, and 40°C and adsorbent dose of 0.5, 1, 2, and 3 g/l at an optimized pH value. The third experimental series was used to study the batch adsorption under optimized conditions ($T = 30^\circ\text{C}$, $m = 1\text{ g/l}$, and $\text{pH} = 2$) with varied initial Cr(VI) concentrations in the range of 50–500 mg/l and to identify the effect of initial Cr(VI) concentration.

For each experiment, a known volume of solution was collected, centrifuged at 3000 r/min, assayed and analyzed calorimetrically with 1.5-diphenylcarbazide using UV–Visible light spectroscopy in order to measure the remaining concentration of Cr(VI) ions in solution. The metal adsorption efficiency of the adsorbent was determined by adsorption capacity as the amount of metal ions of Cr(VI) adsorbed per gram of adsorbent (mg/g).

Adsorption capacity and removal percentage ($A\%$) were calculated from the following equations

$$Q_e = V \frac{C_0 - C_e}{m} \quad (1)$$

$$A(\%) = \frac{C_0 - C_e}{C_0} \times 100 \quad (2)$$

where Q_e is the adsorption capacity (mg/g), V is the volume of solution (l), C_0 is the initial concentration of Cr(VI) (mg/l), C_e is the Cr(VI) concentration at equilibrium (mg/l), and m is the mass of adsorbent (g).

Adsorption kinetic models

Pseudo-first-order and pseudo-second-order kinetic models. Adsorption kinetics was investigated to understand the adsorption dynamic of metal ions onto the adsorbent. Adsorption kinetic is expressed as the solute removal rate that controls the residence time of the adsorbate at the

solid–solution interface (Pandey et al., 2010). So, in order to examine the adsorption mechanism process such as mass transfer and chemical reaction, suitable kinetic models were needed to describe our data. In this study, adsorption kinetic data, including all parameters, were modeled using pseudo-first-order and pseudo-second-order kinetic models; this was envisaged in order to investigate the mechanism and the adsorption process of hexavalent chromium ions onto our activated carbon. The nonlinear pseudo-first-order equation (equation (3)), previously determined by Lagergren (1898), is given as follows

$$q_t = q_e(1 - e^{-k_1 t}) \quad (3)$$

where q_e and q_t are the amounts of hexavalent chromium ions (Cr(VI)) (mg/g) adsorbed at equilibrium and at time t , respectively; k_1 (min^{-1}) is the pseudo-first-order model rate constant; and t (min) is the contact time.

The pseudo-second-order equation (equation(4)) (Ho and McKay, 1999) can be formulated as follows

$$q_t = \frac{q^2 k_2 t}{1 + q_e k_2 t} \quad (4)$$

where k_2 (g/mg min) is the pseudo-second-order rate constant and t (min) is the contact time.

ELOVICH kinetic model. The existence of various chemical groups on the adsorbent has led us to examine the applicability of a model adapted to surfaces such as the Elovich model. Indeed Cr(VI) ions may react on the surface of the adsorbent; this prompts the possibility of a chemical reaction used to control the adsorption mechanism (Tseng and Tseng, 2006). The Elovich kinetic model, represented by equation (5), was applied to each system

$$q = \frac{1}{\beta} \text{Ln}(\alpha\beta t) \quad (5)$$

where α is the initial adsorption rate (mg/g min) and β is the desorption constant (g/mg) associated with the extent of surface coverage and activation energy for chemisorptions.

Adsorption isotherm models

In order to study the mechanism of adsorption and to interpret the relationship between the concentration of the pollutant (adsorbate) and the adsorption capacity of the adsorbent (Naushad, 2014; Wang et al., 2010) at constant temperature, several isotherm models are used to identify the design process (Smith, 1981) and this can provide more information about the capacity of adsorbent. This is usually characterized by the presence of constant values that can affect the nature of the adsorbate–adsorbent surface interaction; we also use this to distinguish the adsorptive capacities of the adsorbent for different pollutants.

In this study, the equilibrium data for the adsorption of Cr(VI) ions onto activated carbon are fitted by seven isotherm models; this is to interpret the equilibrium state for single ion adsorption experiments.

Langmuir. The theoretical basis of Langmuir equation relies on the assumption that there is a finite number of binding sites having a uniform energy and are homogeneously distributed over the adsorbent surface of activated carbon, and there is no interaction between the adsorbed molecules; a saturated layer is formed by the adsorbed molecules and maximum adsorption occurs, so it is assumed that adsorption is of a monolayer type. The mathematical description of the nonlinear equation (equation (6)) is expressed as follows

$$q_e = \frac{Q_m K_L C_e}{1 + K_L C_e} \quad (6)$$

where C_e is the metal residual concentration in solution (mg/l), Q_m is the maximum specific uptake corresponding to sites saturation (mg/g), and K_L is the adsorption equilibrium constant (l/mg) (Donmez and Aksu, 2002).

Freundlich. The Freundlich isotherm was originally empirical in nature, but was interpreted as the adsorption to heterogeneous surfaces or surfaces supporting sites with various affinities. It is assumed that the stronger binding sites are initially occupied. It incorporates two constants: K_F , which corresponds to the binding capacity; and n , which characterizes the affinity between the adsorbent and solute (Bayramoglu et al., 2005). The empirical equation (equation (7)) is presented as follows

$$q_e = K_F C_e^{1/n} \quad (7)$$

Temkin. The Temkin model (Temkin, 1941) is based on the assumption that the heat of adsorption, due to interactions with the adsorbate, decreases linearly over time primarily owing to a decrease in adsorbent–adsorbate interactions during gas-phase adsorption. It is an application of the Gibbs relation for adsorbents whose surfaces are considered energetically homogeneous. Several authors proposed using this model in liquid phase; equation (8) is presented as follows

$$\theta = \frac{q_e}{q_{max}} = \left(\frac{RT}{\Delta Q} \right) \ln(K_T C_e) \quad (8)$$

Dubinin–Raduskovich. Another equation used in the analysis of isotherms was proposed by Dubinin and Raduskovich; this model does not assume the presence of homogeneous surfaces or a constant adsorption potential like those in the Langmuir model. The theory of filling the volume of micropores is based on the fact that the adsorption potential is variable and that the free enthalpy of adsorption is connected by the degree of pore filling. The isotherm is expressed by equation (9)

$$q_e = q_{max} D R e^{(-\beta_{DR} \epsilon^2)} \quad (9)$$

$\varepsilon = RT \ln (1 + (1/C_e))$ potential of Polanyi B and E ($k \text{ J mol}^{-1}$) are related by equation

$$E = \frac{1}{\sqrt{2\beta}} \quad (10)$$

The plot of q_e as a function of ε^2 allows evaluating q_{maxDR} (mg/g) and β . E provides information on the nature of adsorption. In fact, if E is between 8 and 16 (kJ/mol), the process follows an ionic exchange adsorption, whereas for the values of $E < 8$ (kJ/mol), the adsorption process becomes of a physical nature (Ozkaya, 2006).

Redlich–Peterson. This is a three-parameter mono-solute model widely used and cited in literature because of its application for a range of concentrations. It is an empirical model combining the parameters of the Langmuir and Freundlich equations. It has been widely applied to gas-phase adsorption, and by analogy, its expression in liquid phase is given by equation (11)

$$q_e = \frac{A_{RP} C_e}{1 + B_{RP} C_e^{\beta_{RP}}} \quad (11)$$

Under certain conditions, in particular for high solute concentrations in the liquid phase, Redlich–Peterson expression becomes comparable to that of Freundlich

$B_{RP} C_e^{\beta_{RP}} \gg 1$, $q_e = q_{max} A_{RP} C_e^{1-\beta}$, if $\beta = 0$, the isotherm becomes linear (of type C)

Tóth. Tóth (2000) modified the Langmuir equation to reduce the experimental error; it is also a model very often cited and used. It was established for gas-phase adsorption (1962) from the Langmuir isotherm, but also considers that the surface of the adsorbent is not energetically homogeneous; it is therefore of particular interest. The application of the latter is better suited to BET isothermal multilayer adsorption, which is a specific type of Langmuir isotherm and has a very restrictive validity (Khan et al., 1997) in liquid phases; it is generally used as an application of the Langmuir model, close to the empirical model of Redlich–Peterson. The Tóth model is represented by equation (12)

$$q_e = \frac{q_{maxT0} C_e}{\left(1/\kappa_{T0} + C_e^{m_{T0}}\right)^{1/m_{T0}}} \quad (12)$$

The Tóth model is reduced to the Langmuir model when the parameter m_T is equal to unity.

Sips. This three-parameter model is known as the identifier of the main problems associated with the continuous increase in the adsorbent amount with increasing concentrations in the Freundlich equation; Sips (1948) proposed an equation similar to the equation of Freundlich. However, the model has limitations in cases where the concentration is sufficiently high. This isotherm is given by equation (13)

$$q_e = \frac{q_{maxS} K_S C_e^{m_S}}{1 + K_S C_e^{m_S}} \quad (13)$$

Table 1. Approximation of the main constituents of ZRC-AC.

| Constituent analysis (%) | | Type of material | | | |
|--------------------------|--------------------------------|------------------------|--------|-------------|------------------------|
| | | <i>Z. jujuba</i> cores | | | |
| | | Hollocellulose | Lignin | Extractives | Activated carbon (ZRC) |
| | | 39.0 | 31.0 | 7.7 | |
| Proximate analysis | Ash | 4.83 | | | |
| Ultimate analysis | C | 47.06 | | | 85.82 |
| | H | 5.70 | | | |
| | N | 0.24 | | | |
| | O | 42.17 | | | 17.59 |
| Components | MgO | 6.63 | | | 3.79 |
| | Al ₂ O ₃ | 0.840 | | | 18.2 |
| | SiO ₂ | 30.7 | | | 24.8 |
| | P ₂ O ₅ | 6.93 | | | 6.67 |
| | SO ₃ | 5.71 | | | 1.76 |
| | Cl | 1.53 | | | 0.943 |
| | K ₂ O | 3.73 | | | |
| | CaO | 35.0 | | | 31.6 |
| | Fe ₂ O ₃ | 2.71 | | | 0.490 |
| | NiO | 0.407 | | | 1.66 |
| | CuO | 2.03 | | | |
| | ZnO | 1.15 | | | 1.59 |
| | Br | 0.176 | | | |
| | SrO | 0.950 | | | |
| | PbO | 1.58 | | | |
| | Rb ₂ O | | | | 8.39 |
| | ZrO ₂ | | | | 0.0510 |

ZRC-AC: *Z. jujuba* rubidium carbonate-activated carbon.

Results and discussion

Characterization of the “ZRC-AC”

Global chemical analysis. Results of the biochemical analysis and the elemental analysis of the biomass were obtained and are summarized in Table 1; we note that the extracts represent 7.7% of the jujube cores; the carbon content is almost the same as that of oxygen in the raw material; this is due to the significant presence of holocellulose (hemicelluloses and cellulose), on the one hand, and lignin, on the other hand; the nitrogen content in the jujube cores is low; the data also show that the composition of these cores approximates that of wood. These results are confirmed by the visual aspects of jujube cores. Thus, it can be concluded that this material is a lignocellulosic biomass (Benturki, 2008).

XRF analysis of the material, summarized in Table 1, revealed that the components of the biomass are minerals in the form of oxides; for activated carbon synthesized from this lignocellulosic material, the principal inorganic compounds are oxides of silicon, magnesium, calcium, iron, aluminum, and sodium. This is confirmed by the rate of ash, found between 1 and 5%, i.e. 4.83% for the biomass and 4.79% for the activated carbon.

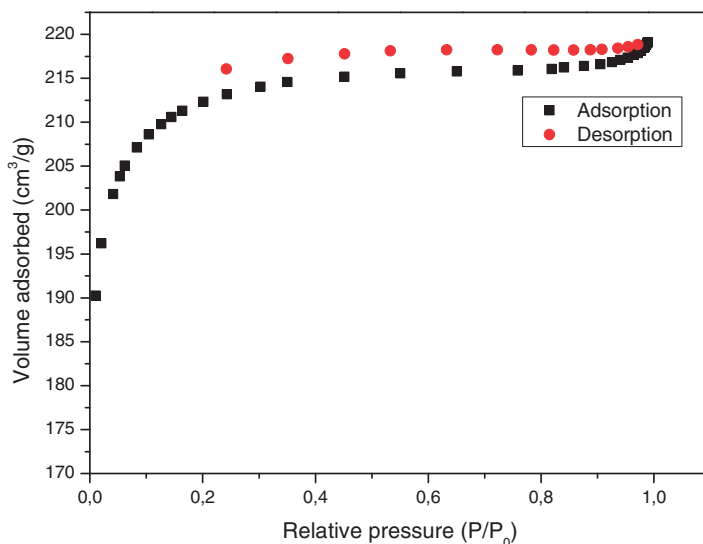


Figure 1. Adsorption/desorption isotherm of N_2 at 77 K on ZRC-AC.

The high content of silicon and calcium present in the biomass is owing to assimilation from the ground.

Rubidium carbonate was used for the activation of the raw biomass; one of the advantages associated with the utilization of the latter reagent is its ability to remove inorganic impurities present in the biomass by dissolution as well as its stability and nonhazardous characteristics; it is clear from Table 1 that the concentration of impurities in the precursor material such as Si and Mg decreased after treatment with rubidium carbonate.

N_2 adsorption–desorption

Figure 1 presents the nitrogen adsorption–desorption isotherm of activated carbon at 77 K; adsorption data were obtained with a relative pressure p/p_0 ranging from 0.01 to 0.989. From Figure 1, the shape of the adsorption isotherm curve exhibits a type I isotherm based on the International Union of Pure and Applied Chemistry (IUPAC) classification (Sing et al., 1985). Type I isotherms are characterized by the presence of micropores; this indicates that our activated carbon is microporous. The adsorption isotherm rises rapidly followed by a flat region, indicating stoppage of the adsorption process since multilayers of the adsorbate cannot be formed; this is primarily due to the close proximity of the pore walls in which adsorption and desorption branches appear almost superimposed and remain parallel to each other over a wide range of relative pressures. This phenomenon also reflects the characteristic behavior of microporous materials (Kennedy et al., 2007). The specific surface area of the activated carbon was calculated by BET equation within a relative pressure range 0.05–0.35; the pore size distribution presented in Figure 2 shows that the activated carbon has a large micropore distribution with a micropore area of $524.71 \text{ m}^2/\text{g}$ compared to the total BET surface area of $608.31 \text{ m}^2/\text{g}$; the micropore volume was also calculated at $0.2916 \text{ cm}^3/\text{g}$ compared to a maximum pore volume of $0.3388 \text{ cm}^3/\text{g}$ and with a median pore diameter of 10.2411 \AA . The latter coincides well with the classification categories of

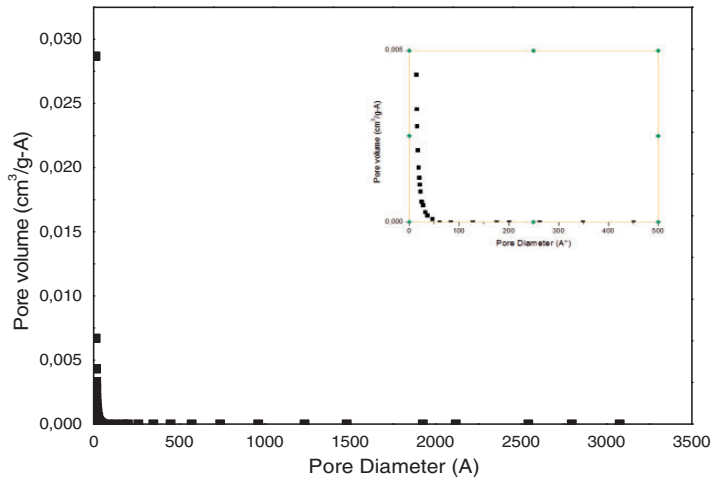


Figure 2. Pore size distribution of ZRC-AC.

Table 2. Textural characteristics of the prepared *Z. jujuba* rubidium carbonate-activated carbon (ZRC-AC).

| Physical properties | Volume |
|--|--------|
| BET surface area (m ² /g) | 608 |
| Total volume V_t (cm ³ /g) | 0.33 |
| Microporous volume (cm ³ /g) | 0.29 |
| Mesoporous volume V_{meso} (cm ³ /g) | 0.04 |
| Median pore diameter (Å°) | 10.24 |

IUPAC where by micropores (< 2 nm), mesopores (2–50 nm), and finally macropores (> 50 nm); therefore, it can be concluded that the high adsorption capacity of our activated carbon despite the low surface area BET can be interpreted by the presence of a large distribution of micropores that adsorbed chromium ions with ionic radius of 0.044 nm. The pore structure parameters are presented in Table 2.

SEM

SEM is a very useful tool to examine the surface structure and morphological feature of biomass and activated carbon. Figure 3 displays SEM images of the surface structure and morphology of our materials, so the effect of activation and carbonization on the pore distribution and morphology of activated carbon was clearly demonstrated while significant differences in surface morphologies of our samples were also observed.

Figure 3 illustrates the presence of a large number of pores on the surface of our materials; the latter products tend to possess porous, rough surfaces, with distinct walls resulting from subjecting the material to chemical and thermal activation processes. The creation of micro and mesopores was the result of the volatilization of some materials such as lignin and other organic compounds present in *Z. jujuba* cores during impregnation and thermal

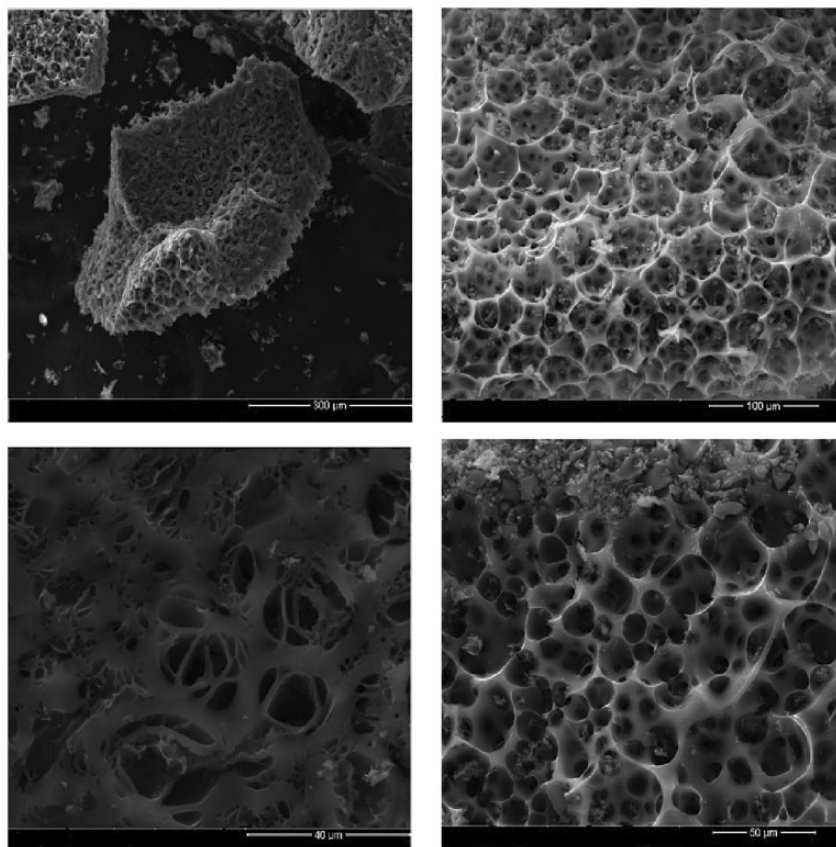


Figure 3. SEM micrographs of ZRC-AC.

activation; thus, causing the opening of the pores and consequently creating micro and mesopores. It can be seen that the formation of craters, whereby the diameter at the mouth of the pore is at macropore levels and is larger than the interior of the pore, can be a consequence of chemical activation; as a result, an effective adsorbent which has an homogenous structure and deep pores with large surface areas and pore volumes is obtained. This was previously cited in other works whereby similar observations were found (Sekaran et al., 2013; Yang et al., 2015).

FTIR spectroscopy

Surface chemistry is the main parameter for determining the adsorption capacity of activated carbon; the prepared activated carbon had a high content of carbon and a low content of oxygen. Functional groups on the activated carbon are determined by the pH of the activated carbon (pH_{pzc}) which was measured at 9; however, more information about the nature of these functional groups are obtained using FTIR analysis. This has been clearly demonstrated in Figures 4(a) and (b) and 5; the latter shows superimposed spectra of our

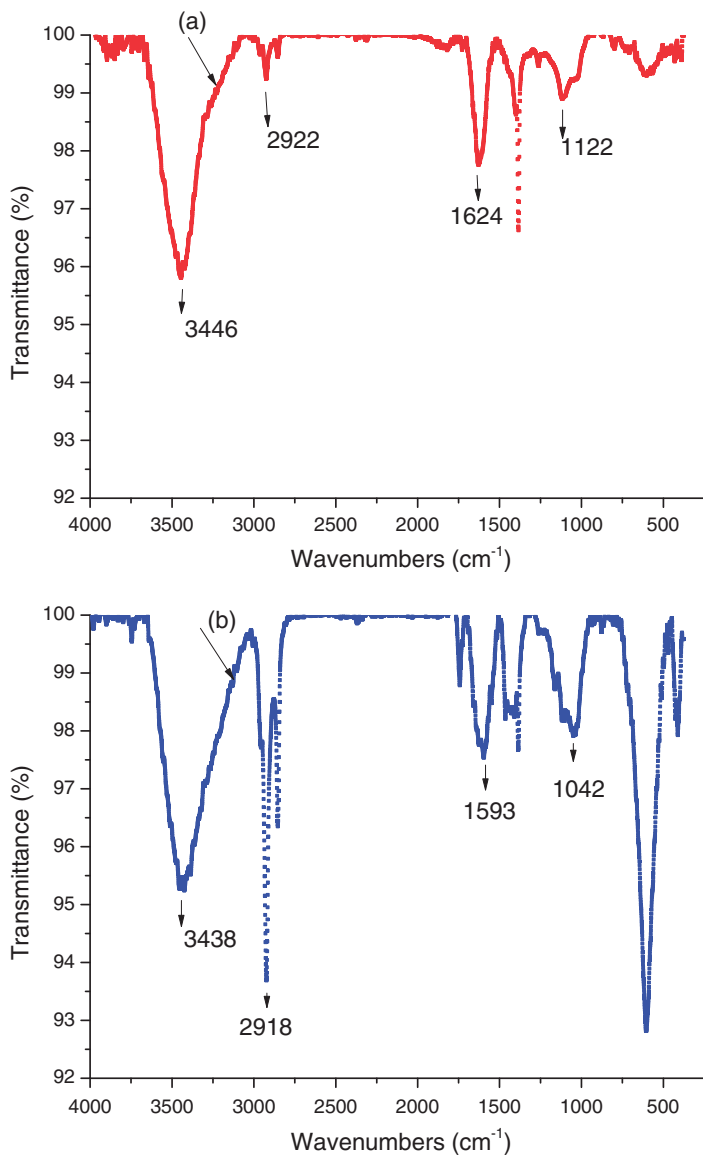


Figure 4. FTIR spectra of ZRC-AC (a) and the Cr(VI)-loaded ZRC-AC, Cr(VI) (b).

materials. The broad bands at 3423 cm⁻¹ are attributed to (O–H) stretching vibrations as well as amino (N–H) groups; the absorption peaks at 2922 and 2852 cm⁻¹ are attributed to the (C–H) asymmetric and symmetric stretching vibrations, respectively. The peak at 1624 cm⁻¹ is attributed to (C = C) vibration and the peak at 1384 cm⁻¹ is assigned to the bending vibrations of –CH₃. The peak at 1122 cm⁻¹ corresponds to C–O stretching vibrations; finally, the peak at 619 cm⁻¹ is attributed to C–H stretching vibrations as previously assigned in literature (Alshehri et al., 2014; Burg et al., 2002).

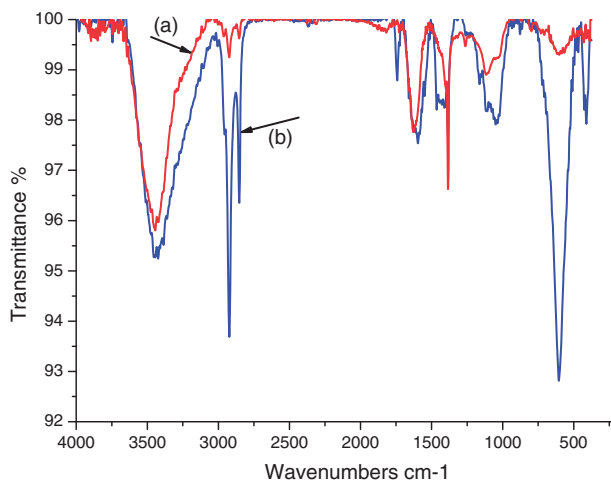


Figure 5. FTIR spectra of “ZRC-AC” (a) before adsorption and (b) after adsorption of hexavalent chromium.

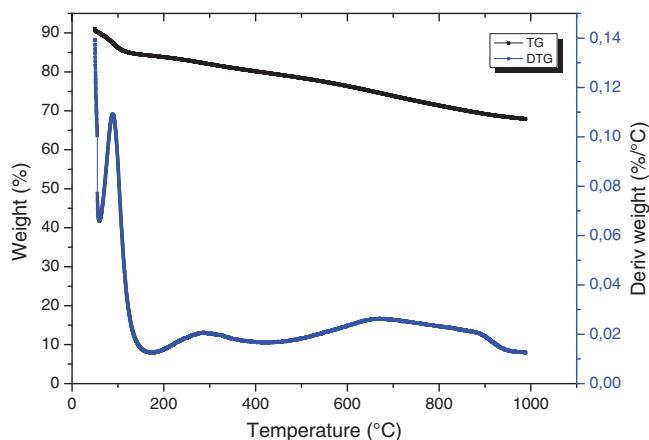


Figure 6. Thermogravimetric and derived thermogravimetric spectra TG/DTG of ZRC-AC.

TGA

The protocol of TGA is detailed as above. These measurements were made under nitrogen atmosphere to avoid combustion of the activated carbon. The corresponding thermograms are shown in Figure 6.

A first loss of mass is observed at about 100°C, which must correspond to the loss of moisture content of the activated carbon (53.89%); this quantity of water or small adsorbed molecules is surely related to their higher surface area. From this temperature, the mass slope becomes relatively high; the mass loss at moderate temperatures corresponds to the decomposition of carboxylic groups (150–400°C) and lactones (350–600°C). This coincides with the presence of cellulose at 300°C as shown in the figure (deriv. weight (%/°C));

however, the increased mass loss starting at 600°C, as well as the presence of curves of the derived weight as a function of temperature at 650 and 900°C, correspond well to the presence of phenols, carbonyls, and basic groups. So, it can be observed that the mass slope is very high which can be associated with the decomposition of weak acids to CO and CO₂ gas (Driel et al., 1983; Zielke et al., 1996).

Effect of batch adsorption parameters

Effect of contact time and initial pH of solution. pH is one of the most important environmental factor used to determine the adsorption of heavy metal ions; the value strongly influences the properties of both adsorbates and adsorbents such as the ionic state of functional groups present on the adsorbent as well as the chemical properties of the studied metal in solution (Mohanty et al., 2006); for this reason, the pH affects not only the degree of ionization and specifications of the adsorbate, but also the surface charge of the adsorbent during reaction (Babel and Kurniawan, 2004), so the effect of pH directly impacts the electrostatic interactions between the adsorbate and adsorbent's surface. In order to study the effect of pH on adsorption of Cr(VI) ions by "ZRC-AC," a series of kinetic experiments for each value of pH (1–6) were studied at constant Cr(VI) concentration (100 mg/l) and "ZRC-AC" (1 g/l). The experiments were performed in a conical flask (250 ml) and placed in a mechanical shaker equipped with a thermostatic water bath set between 180 and 200 bpm at 30°C. The results are illustrated in Figure 7.

Figure 7(a) shows the effect of solution pH on the removal percentage of Cr(VI) following kinetic adsorption; the amount of adsorbed chromium (q_t , mg/g) at first presents a rapid increase with increasing contact time; it has also been noticed that the maximum removal percentage of Cr(VI) was observed at pH = 2. The equilibrium time reached 360 min; also, as the contact time increased from 0 to 360 min, the amount of Cr(VI) ions, adsorbed on "ZRC-AC," was almost constant beyond 360 min; this means that state of equilibrium was achieved as a result of lack in active sites used for further adsorption.

We can observe from Figure 8 that decreasing the pH from 6 to 2 leads to an increase in adsorption from 27.2 to 62.08 mg/g, so we can conclude that pH = 2 is the best optimum pH value for the highest removal efficiency or adsorption of chromium ions on activated carbon; although previous works by other scientists such as those of Garg et al. (2007), Kiran et al. (2007), and Malkoç et al. (2006) used different adsorbents, they also found that pH = 2 was an optimum pH value for the maximum adsorption of Cr(VI) ions; this process is well observed in acidic media. Similar results were observed by El-Shafey (2005) who suggested the use of modified rice husk as adsorbent for the removal of chromium ions from wastewater. Our results are also in agreement with previous studies by Liu et al. (2014) and Karthikeyan et al. (2005); the former study affirmed that the adsorption phenomenon, as a function of pH, is dependent on (i) Cr(VI) species, (ii) their solubility in solution, and (iii) the overall surface charge of the activated carbon (Gueye et al., 2014).

Different forms of hexavalent chromium Cr(VI) exist in aqueous solutions, for example, CrO_4^{2-} , HCrO_4^- , and $\text{Cr}_2\text{O}_7^{2-}$; the stability of Cr(VI) ions is dependent on pH of solution. In pH ranging from 2 to 6, the predominant form of Cr(VI) ions is those mentioned earlier. It is well known that the dominant form of Cr(VI) at pH = 2 is HCrO_4^- , so, pH_{pzc} , previously determined in Figure 8, revealed that "ZRC-AC" ($pH_{pzc} = 9$) possessed basic properties.

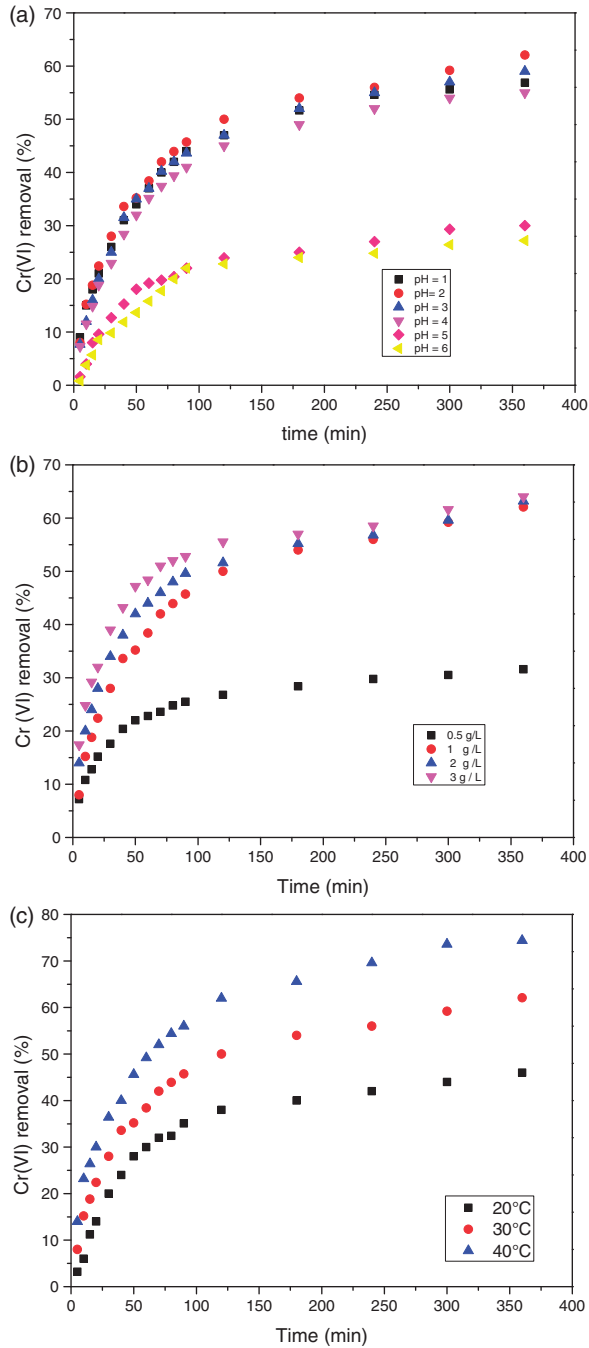


Figure 7. Effect of (a) contact time and initial solution pH, (b) of adsorbent dose, (c) temperature on Cr (VI) removal percent by ZRC-AC (Cr(VI) concentration= 100 mg/l, adsorbent dose = 1 g/l, agitation rate, 200 bpm and T = 30°C for (a) and (b)).

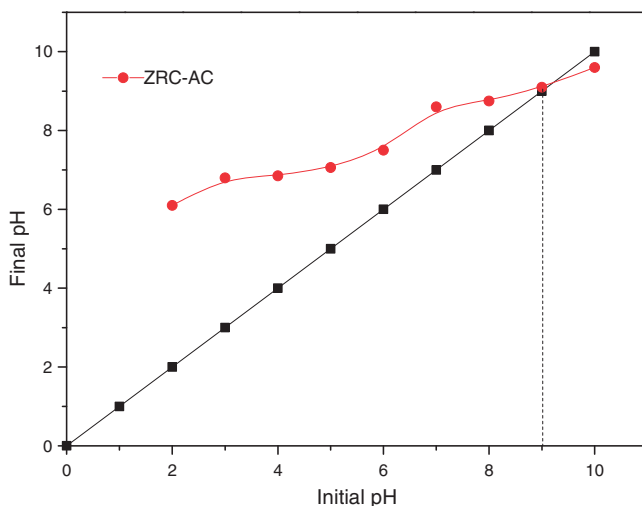


Figure 8. Determination of pH_{pzc} of ZRC-AC. ZRC-AC: *Z. jujuba* rubidium carbonate-activated carbon.

When the pH of solution is less than pH_{pzc} , the adsorption of anionic species is promoted, whereas, when pH of solution is greater than pH_{pzc} , the adsorption of cationic species is favorable; based on this, it is well described that:

- (i) At $pH = 1$, although the medium is acidic, a small rate of elimination has been noticed; at such pH, more protons are available which can promote the reduction of Cr(VI) to Cr(III). The cationic ions interact with the protonated surface of activated carbon via an electrostatic repulsion phenomenon as a result of competition between protons, Cr (III) species, and the adsorption surface active sites (Liu et al., 2014).
- (ii) At $pH = 2$, the dominant form of chromium is $HCrO_4^-$, so, at lower pH values, a large number of H^+ ions exists in the solution medium; as a result, the surface protonation of activated carbon leads to the formation of positively charged sites. These protons interact with chromium atoms by an electrostatic attraction phenomenon so that $HCrO_4^-$ is adsorbed on carbon thus causing an increase in chromium adsorption.
- (iii) At $2 > pH > 6$, the gradual decrease in the rate of adsorption is due to the coexistence of $Cr_2O_7^{2-}$ and CrO_4^{2-} with $HCrO_4^-$ in the solution medium; thus, causing competition on the adsorption sites. Furthermore, similar results have also been reported by other investigators (Rao et al., 2002; Ucum et al., 2002).

The decrease in chromium adsorption resulting from the increase in pH of solution can be explained by the abundance of OH^- ions in solution which in turn can compete with the chromate and hydrogen chromate ions for adsorption; as a result, an electrostatic repulsion phenomenon takes place. The electrostatic interactions can give rise to chemisorptions as explained by equations (14) to (16) (Liu et al., 2014). The theoretical distribution of the predominant chemical species of Cr(VI) is presented in Figure 9(a) (Barrera-Diaz et al., 2012)



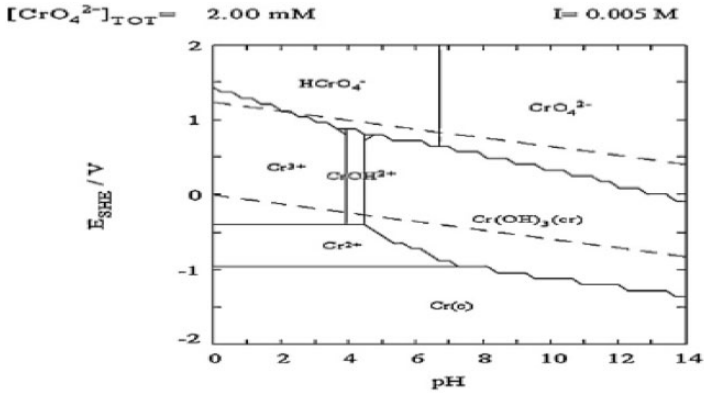


Figure 9. Pourbaix diagram for Cr chemical species in aqueous solution ($[\text{CrO}_4^{2-}] = 2.00 \text{ mM}$, $I = 0.005 \text{ M}$, and $T = 25^\circ\text{C}$).



Effect of contact time and adsorbent dose of activated carbon on the adsorption of hexavalent chromium. The effect of adsorbent dosage on Cr(VI) adsorption was investigated by varying the amount of activated carbon from 0.5 to 3 g/l. Figure 7(b) illustrates the variation of removal percentage of Cr(VI) at different adsorbent doses; generally, experimental data showed that the removal percentage of Cr(VI) increased from 31.6 to 64% at an initial Cr(VI) concentration of 100 mg/l, while the adsorbent mass increased from 0.5 to 3 g/l. This may be due to an increase in the availability of active sites when there is more amount of adsorbent dose. However, since there were no large differences observed between the adsorption percentage of Cr(VI) at adsorbent concentration of 3 and 1 g/l, we decided to take into account the most economical approach where it was considered that the adsorbent dose of 1 g/l is an optimum dose for our studies.

Effect of temperature on adsorption of Cr(VI) onto Z. jujube rubidium carbonate activated carbon. Figure 7(c) illustrates that the increase in diffusion rate of Cr(VI) ions during the process of external mass transport with respect to temperature (Meena et al., 2008) favors an increase in removal percentage from 46 to 74.4%. This phenomenon could be explained by the dispersion of Cr(VI) ions and the increase in the number of adsorption sites resulting from the rupture of the internal bonds near the surface sites; however, the decrease in removal percentage at low temperature can be attributed to the low kinetic energy of Cr(VI) ions heading toward the active sites of the adsorbent, consequently, this leads to ion agglomeration and thereby minimizing the interaction between the adsorbate and the active sites. This is primarily due to the microporous nature of the activated carbon.

Relationship between the effect of temperature and adsorbent dose: Figure 10 indicates that increasing the adsorbent dose from 0.5 to 3 g/l results in a decrease of adsorption capacity per unit mass, this was from 62 to 16.53 mg/g at 20°C , 63.2 to 21.33 mg/g at 30°C , and 97.2

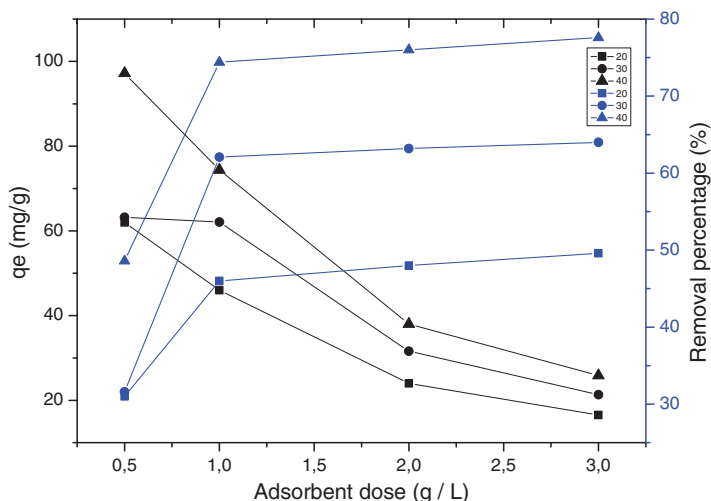


Figure 10. Variation amount of metal adsorbed per unit mass and removal percentage of Cr(VI) as a function of adsorbent dose at different temperatures (20, 30, and 40°C) (Cr(VI) concentration= 100 mg/l and agitation rate of 200 bpm).

to 25.86 mg/g at 40°C, whereas the chromium removal percentage reached 49.6% at 20°C, 64% at 30°C, and 77.6% at 40°C. The rapid increase in removal percentage $A\%$ with respect to an elevated adsorbent dose can be explained by the presence of more adsorption sites and larger microporous surface areas; the sharp decrease in adsorption capacity can be due to (i) the instauration of adsorption sites throughout the adsorption reaction (Rao et al., 2008) and (ii) the reduction in adsorbate/adsorbent surface areas (Liu et al., 2010); in other words, the amount of metal adsorbed per unit mass of adsorbent decreased with increasing the adsorbent dose; however, the removal percentage (%) increased with increasing the adsorbent dose (Zhang et al., 2010).

Modeling of batch adsorption kinetic data

All kinetic experimental data were fitted by pseudo-first-order, pseudo-second-order, and Elovich models according to the equations cited above; all plots are shown in Figures 11 and 12. The results and kinetic parameters including first-order rate constant k_1 , experimental and calculated equilibrium adsorption capacity, second-order rate constant k_2 , and correlation coefficient (R^2) are presented in Table 3 in order to enable us understand the adsorption kinetic process and to find the best fitted model for our experimental data; so, in order to evaluate the best fitting model, both nonlinear chi-square test analysis (χ^2) and correlation coefficients (R^2) calculations were performed (Zhang et al., 2010). For all adsorption factors, the application of a pseudo-first-order model gave small value correlation coefficient (R^2), a large (χ^2), and a large difference between the theoretical and calculated adsorption capacity at equilibrium; all of these results revealed that this model is not applicable to the kinetic adsorption of Cr(VI) ions onto activated carbon when compared with a pseudo-second-order model; the latter showed an experimental equilibrium adsorption capacity (q_e (exp))

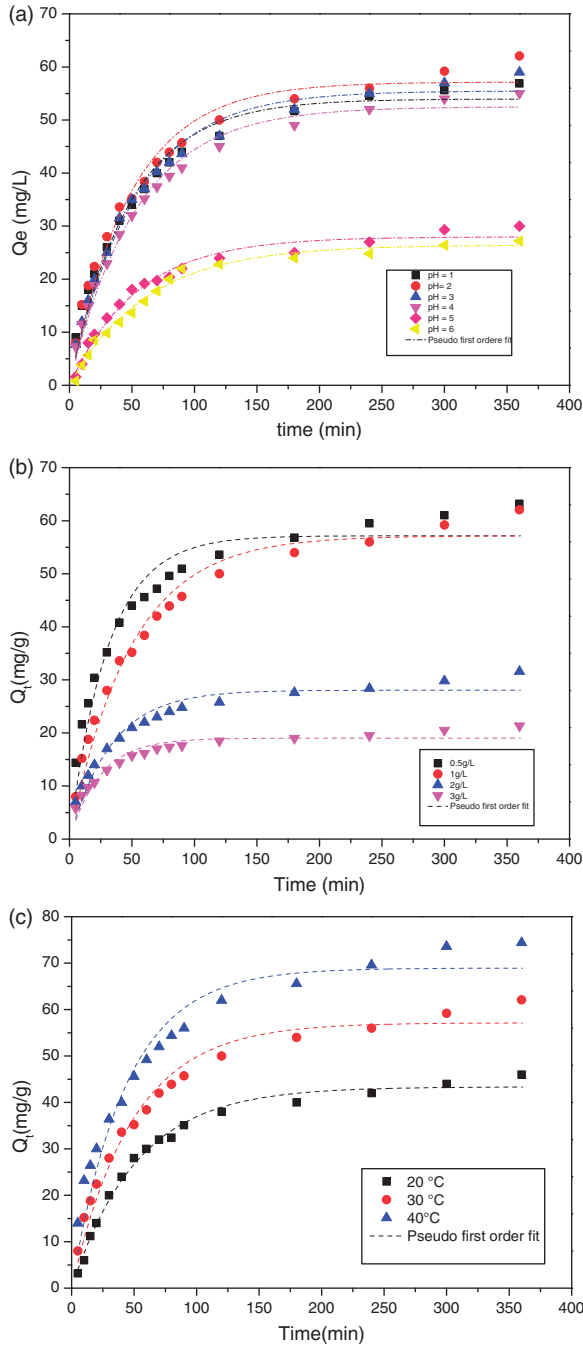


Figure 11. Adsorption of chromium as a function of time (a) at varied solutions pH, (b) at varied adsorbent dose, and (c) at varied temperatures for the kinetic pseudo-first-order model and (d), (e), (f) for the kinetic pseudo-second-order model (chromium concentration = 100 mg/l, stirring speed = 200 r/min).

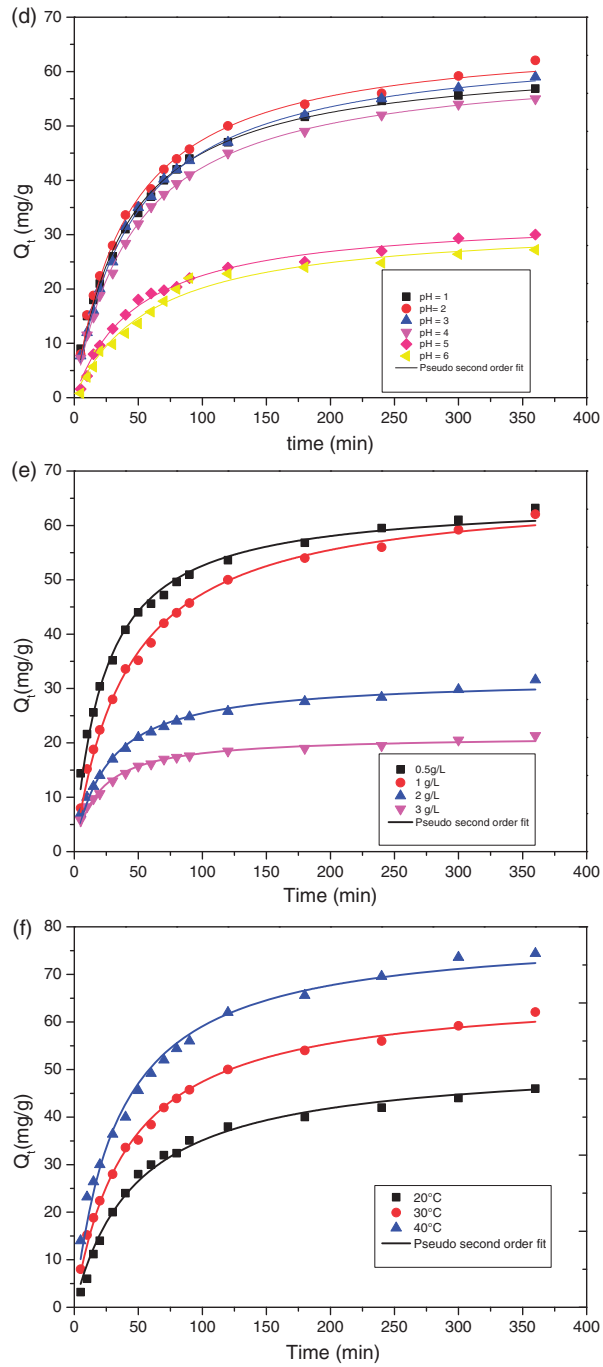


Figure II. (continued).

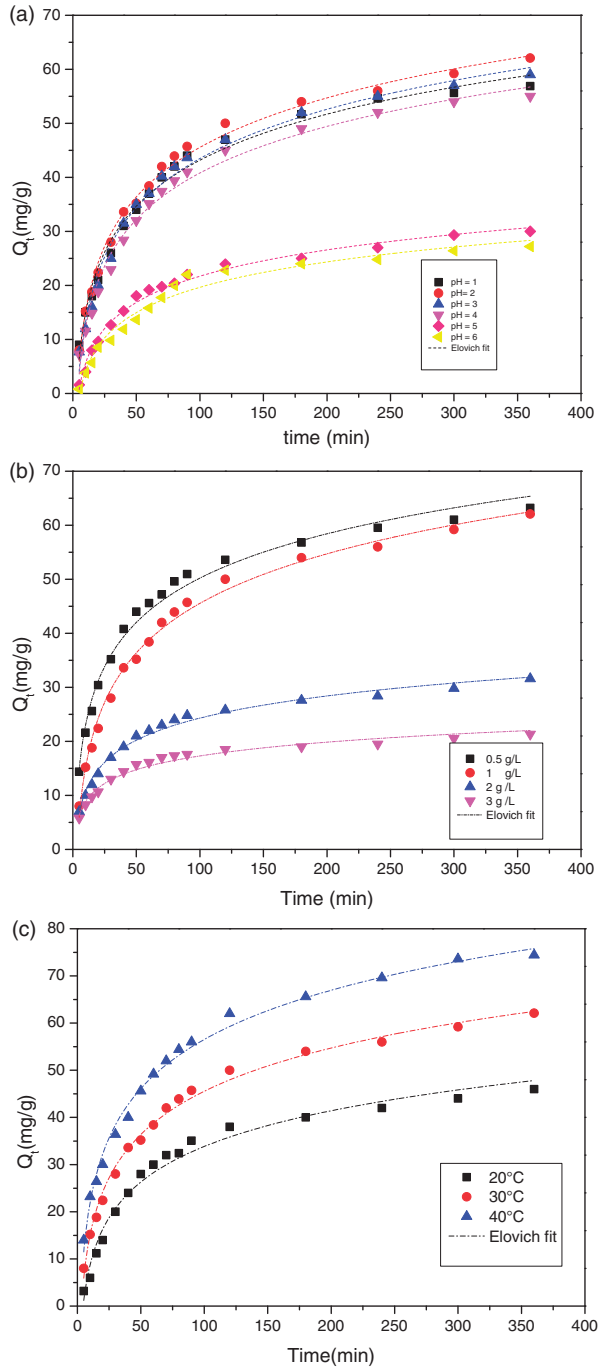


Figure 12. Adsorption of chromium as a function of time (a) at varied solutions pH, (b) at varied adsorbent dose, and (c) at varied temperatures for the kinetic Elovich model (chromium concentration = 100 mg/l, stirring speed = 200 r/min) Pseudo-first-order, pseudo-second-order, and Elovich models rate constants for pH values and adsorbent doses.

Table 3. Pseudo-first-order, pseudo-second-order, and Elovich parameters.

| pH values | Pseudo-first-order model | | | | | Pseudo-second-order | | | Elovich | | | |
|------------------------------|--------------------------|-----------------------------|-------|--------------------|----------|--|-------|--------------------|----------------|--------------------|-------|-------------------------|
| | q_e (exp) (mg/g) | K_1 (min^{-1}) | R^2 | q_e (cal) (mg/g) | χ^2 | $K_2 \times 10^{-4}$ (min^{-1}) | R^2 | q_e (cal) (mg/g) | χ^2 | q_e (cal) (mg/g) | R^2 | $\chi^2 \times 10^{-2}$ |
| 1 | 56.88 | 0.020 | 0.972 | 53.97 | 0.156 | 3.9 | 0.995 | 62.90 | 0.576 | 58.92 | 0.987 | 7.063 |
| 2 | 62.08 | 0.020 | 0.969 | 57.15 | 0.425 | 3.63 | 0.995 | 66.91 | 0.348 | 62.48 | 0.992 | 0.256 |
| 3 | 59 | 0.019 | 0.983 | 55.48 | 0.223 | 3.35 | 0.998 | 65.64 | 0.671 | 60.32 | 0.988 | 2.88 |
| 4 | 55 | 0.018 | 0.986 | 52.50 | 0.119 | 3.41 | 0.998 | 62.26 | 0.846 | 56.73 | 0.985 | 5.27 |
| 5 | 30 | 0.018 | 0.980 | 27.98 | 0.145 | 6 | 0.99 | 33.51 | 0.367 | 30.69 | 0.989 | 1.55 |
| 6 | 27.2 | 0.016 | 0.988 | 26.43 | 0.022 | 5.14 | 0.98 | 32.32 | 0.811 | 28.33 | 0.97 | 4.5 |
| Adsorbent dose (g/l) at 30°C | | | | | | | | | | | | |
| 0.5 | 63.2 | 0.032 | 0.931 | 57.17 | 0.636 | 6.6 | 0.991 | 64.78 | 0.038 | 65.37 | 0.987 | 7.2 |
| 1 | 62.08 | 0.020 | 0.969 | 57.15 | 0.425 | 3.6 | 0.995 | 66.91 | 0.348 | 62.48 | 0.992 | 0.25 |
| 2 | 31.6 | 0.030 | 0.933 | 28.06 | 0.446 | 12.2 | 0.988 | 31.94 | 0.003 | 31.87 | 0.988 | 0.228 |
| 3 | 21.33 | 0.040 | 0.919 | 19.02 | 0.280 | 26 | 0.986 | 21.34 | 4,68 10^{-6} | 22.01 | 0.973 | 2.10 |

that was in good agreement with the calculated one. It is also clear that (R^2) values are more than 0.98; this clearly indicates that the data are well fitted by a pseudo-second-order model instead of a pseudo-first-order model.

For the Elovich kinetic model, constants α and β were obtained from the table and extracted from origin, whereby $a = \alpha$ and $b = \beta$ for the purpose of calculating q_e . These values are reported in Table 3. The correlation coefficients (R^2) are higher than 0.98, which are comparable with other correlation coefficients obtained from pseudo-second-order model. This indicates the applicability of this model for the analysis of our experimental data. The rate-limiting step in this process is the chemical sorption between Cr(VI) and the active sites on our adsorbent; the energy of activation in our sorption process increases accordingly.

Modeling of batch adsorption isotherm data

The aim of this work is to find several models that can be used to describe the experimental data obtained from the adsorption process; for this reason, the equilibrium data were modeled with two-parameter equations by applying the concept of four models (Langmuir, Freundlich, Temkin, and Dubinin–Raduskovich), and three-parameter equations, by applying the concept of three models (Redlich–Peterson, Tóth, and Sips). These calculations are performed in order to find the model that can best describe, with precision, the experimental results of our adsorption process, also to compare the theoretical adsorption isotherms with the experimental ones; these protocols shall also provide us with more insights regarding the behavior of chromium in solution. In order to compare models, several parameters were taken into account, including the correlation coefficient (R^2), which reflects the good fit between the experimental data and the isotherm equation, as well as the average percentage error (APE), calculated following equation (17), which can also be used to express the fit between the experimental and theoretical values of adsorption

capacities utilized for plotting the isotherm curves

$$\text{APE}(\%) = \frac{\sum_{i=1}^N |(q_e)_{\text{experimental}} - (q_e)_{\text{predicted}}| / (q_e)_{\text{experimental}}}{N} \times 100 \quad (17)$$

where N is the number of experimental data.

Two-parameter models

Langmuir isotherm. The fitting results and the Langmuir constant q_m and k_L obtained from the adsorption of Cr(VI) onto activated carbon at different temperatures are summarized in Table 4. The lower correlation coefficient obtained from Langmuir model at 20 and 30°C suggested that this model was not appropriate for the Cr(VI) adsorption. On the other hand, it is clear that the correlation coefficient at 40°C was better; thus, the Langmuir model provided a better fit at this temperature. However, this model did not perfectly describe the equilibrium data owing to the elevated APE obtained.

The second information that can be extracted from this model was the favorable adsorption nature of our adsorbate material; this was previously described by Hall et al. (1966) whereby $R_L = 1/(1 + k_L C_0)$ whereby k_L is the Langmuir constant and C_0 is the initial concentration of the adsorbate in solution. $0 < R_L < 1$ indicates a favorable adsorption, linear ($R_L = 1$), on the other hand, $R_L > 1$ makes the process unfavorable or irreversible ($R_L = 0$). In our case, the calculated R_L at all three temperatures were less than 1 and greater than 0, therefore, suggesting a favorable adsorption.

Temkin isotherm. The adsorption data of Cr(VI) onto activated carbon were analyzed using Temkin isotherm model. The value of surface coverage θ for all three temperatures was calculated using the theoretical maximum adsorption capacity (theoretical q_{max}) obtained from the Langmuir or from the Freundlich models.

The parameters of Temkin model are regrouped in Table 4; the value of θ is higher than 0.68 for all three temperatures; however, the lower correlation coefficient obtained, in conjunction with the presence of a higher APE, makes the Temkin isotherm not fit to adequately describe the adsorption isotherm of Cr(VI) onto activated carbon; the mean values of the APE at 20, 30, and 40°C are 4.57, 9.68, and 6.55%, respectively.

Dubinin–Raduskovich isotherm. The high value of correlation coefficient ($R^2 \geq 0.994$, Table 4) confirms that our material is microporous despite the presence of an elevated APE and a closer approximation between the theoretical and experimental values of the maximum adsorption capacity at all three temperatures (20, 30, and 40°C).

Three-parameter models

The three-parameter equations of Redlich–Peterson, Sips, and Tóth models were tested in our study for the purpose of modeling the equilibrium adsorption data. The values of parameters obtained using nonlinear fitting analyses are regrouped in Table 4.

The Tóth model fits well with the adsorption isotherm of hexavalent chromium at different temperatures; the correlation coefficient is also good ($R^2 > 0.992$). The low value of

Table 4. Values showing the constants of the two- and the three-parameter models and correlation coefficients.

| Model | Parameters | Cr(VI) | | |
|---------------------|--|-----------------------|----------------------|--------|
| | | 20°C | 30°C | 40°C |
| Langmuir | q_{mpredict} (mg/g) | 96 | 126 | 166.4 |
| | q_{mL} (mg/g) | 124.25 | 159.35 | 196.38 |
| | K_L (l/mg) | 0.012 | 0.016 | 0.021 |
| | R^2 | 0.987 | 0.978 | 0.993 |
| Freundlich | APE (%) | 3.97 | 8.95 | 6.57 |
| | K_F (l/mg) | 10.48 | 16.66 | 22.73 |
| | R^2 | 0.943 | 0.913 | 0.948 |
| Temkin | APE (%) | 11.16 | 16.46 | 13.92 |
| | a | 0.111 | 0.137 | 0.202 |
| | b | 27.78 | 36.12 | 42.42 |
| | R^2 | 0.978 | 0.964 | 0.987 |
| Dubinin–Raduskovich | APE (%) | 4.57 | 9.68 | 6.55 |
| | q_{mD} (mg/g) | 110.64 | 146.20 | 178.49 |
| | R^2 | 0.984 | 0.996 | 0.995 |
| Tóth | APE (%) | 7.01 | 2.50 | 7.55 |
| | q_{mT} (mg/g) | 104.05 | 131.61 | 180.99 |
| | K_T | $1.536 \cdot 10^{-4}$ | $2.44 \cdot 10^{-5}$ | 0.0056 |
| | m_T | 1.894 | 2.41 | 1.30 |
| | R^2 | 0.993 | 0.995 | 0.994 |
| Sips | APE (%) | 3.55 | 4.03 | 4.43 |
| | q_{mS} (mg/g) | 110.22 | 133.94 | 181.77 |
| | K_S (L ^m mg ^{-m}) | 0.0043 | 0.0015 | 0.012 |
| | m_S | 1.307 | 1.724 | 1.204 |
| | R^2 | 0.990 | 0.997 | 0.995 |
| Redlich–Peterson | APE (%) | 3.86 | 11.80 | 4.15 |
| | A | 1.058 | 1.8 | 3.65 |
| | B | $9.65 \cdot 10^{-4}$ | 0.00129 | 0.011 |
| | β | 1.358 | 1.367 | 1.087 |
| | R^2 | 0.987 | 0.993 | 0.994 |
| | APE (%) | 2.86 | 4.60 | 3.51 |

APE: average percentage error.

APE in conjunction with the close approximation between the experimental and theoretical maximum adsorption capacity (Table 4) also indicates that the Tóth model provides an excellent description for our experimental results when compared to the Sips model in which case lower correlation coefficient ($R^2 < 0.998$) and higher APE were obtained.

The experimental results of our adsorption isotherm were also fitted using the Redlich–Peterson model; the results are summarized in Table 4. The correlation coefficient and APE (3.65%) provide a satisfactory result in terms of data fitting.

When comparing two-parameter models with three-parameter models, the Tóth model stands out; this is due to the lower APE value (4%). The two-parameter models, i.e.

Table 5. Comparison between the adsorption capacities of various activated carbons and our “ZRC-AC” for Cr(VI) removal.

| Adsorbent | Adsorption capacity (mg/g) | Adsorbent dose (g/l) | Reference |
|--------------------------------|----------------------------|----------------------|------------------------------|
| Coconut shell carbon | 10.88 | 1.5 | Babel and Kurniawan (2004) |
| Sawdust-activated carbon | 3.46 | 4 | Hamadi et al. (2001) |
| Almond | 10.62 | 8 | Dakiky et al. (2002) |
| Cactus | 7.08 | 8 | Dakiky et al. (2002) |
| Raw rice bran | 0.07 | 10 | Oliveira et al. (2005) |
| Sunflower stem | 4.9 | 4 | Jain et al. (2009) |
| Coaly activated carbon | 8.77 | 5 | Wu et al. (2009) |
| Sulfur acid-modified waste | 7.49 | 2 | Ghosh (2009) |
| Fe-modified <i>T. natans</i> | 11.83 | 1.5 | Liu et al. (2010) |
| Olive bagasse | 126.67 | – | Demiral et al. (2008) |
| Hazelnut shell | 170.0 | – | Kobyas (2004) |
| Tires | 58.50 | – | Hamadi et al. (2001) |
| Bael fruit shell | 17.27 | – | Anandkumar and Mandal (2009) |
| <i>T. arjuna</i> nuts | 28.43 | – | Mohanty et al. (2005) |
| Bituminous | 10.53 | – | Lima et al. (2011) |
| Rubber wood sawdust | 44.05 | – | Karthikeyan et al. (2005) |
| Coconut tree sawdust | 3.46 | – | Selvi et al. (2001) |
| Groundnut husk | 7.0 | – | Dubey and Gopal (2007) |
| Tamarind hull | 85.91 | – | Verma et al. (2006) |
| <i>C. equisetifolia</i> leaves | 17.2 | – | Ranganathan (2000) |
| Tamarind wood | 28.02 | – | Acharya et al. (2009) |
| Longan seed | 35.02 | 0.3 | Yang et al. (2015) |
| <i>Z. jujuba</i> cores | 196.38 at 40°C | 1 | This study |

ZRC-AC: *Z. jujuba* rubidium carbonate-activated carbon.

Dubinin–Raduskovich, Langmuir, and Freundlich, are better than the Sips model; therefore, the following trend can be used to summarize the best models used to describe the adsorption equilibrium isotherm of Cr(VI) onto activated carbon

Tóth > Dubinin–Raduskovich > Redlich–Peterson > Langmuir > Sips > Temkin > Freundlich

In summary, the importance of our work is to study and compare as many isotherms as possible in order to get as much information about the nature of the adsorption process of Cr(VI) onto our activated carbon. It is also apparent that the three-parameter models are better used to explain the adsorption process when compared to two-parameter models; this observation has been previously described by Hamdaoui and Naffrechoux (2007). Moreover, three-parameter models were developed to address deficiencies associated with the two-parameter models (Khan et al., 1997; Mullah and Robinson, 1996; Ozkaya, 2006; Vijayaraghavan et al., 2006)

A comparison between the maximum adsorption capacity of Cr(VI) ions onto “ZRC-AC” and other adsorbents has been performed and the results are regrouped in Table 5.

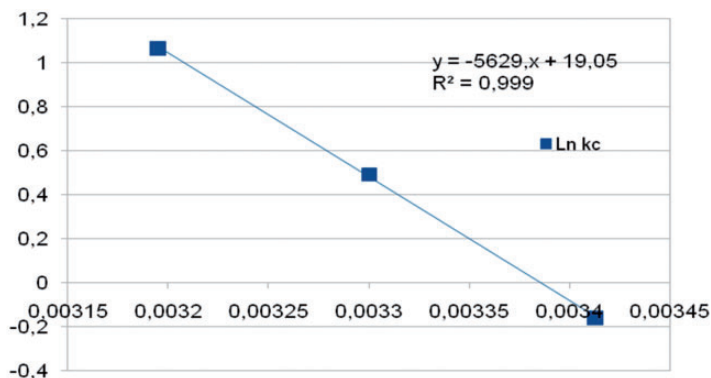


Figure 13. Plot of $\ln K_c$ versus $1/T$.

Thermodynamic parameters

Thermodynamic parameters such as enthalpy (ΔH° , kJ/mol), standard entropy (ΔS° , kJ/(mol K)), and changes in the Gibbs free energy (ΔG° , kJ/mol) were calculated in order to understand the adsorption process; the following equations have been taken into account

$$K_c = \frac{C_0 - C_e}{C_e} \quad (18)$$

$$\ln K_c = -\frac{\Delta H}{RT} + \frac{\Delta S}{R} \quad (19)$$

$$\Delta G = -RT \ln K_c \quad (20)$$

$$\Delta G = \Delta H - T\Delta S \quad (21)$$

where K_c is the equilibrium constant, R (8.134 J/(mol K)) is the gas constant, and T (K) is the absolute temperature. The data of $\ln K_c$ versus $1/T$ were fitted using the Van't Hoff plot (Figure 13); from this plot, values of ΔH and ΔS were obtained from the slope and the point of intercept. The straight line, which does not pass through origin, shows a good linear relationship with both values of slope and point of intercept determined at -5629.25 and 19.05 ; the correlation coefficient $R^2 = 0.999$.

The thermodynamic values (ΔH° , kJ/mol), (ΔS° , kJ/(mol K)), and (ΔG° , kJ/mol) for the adsorption of Cr(VI) ions onto "ZRC-AC" were calculated using the equations above; the results are summarized in Table 6. The positive values of ΔH° revealed that the adsorption of Cr(VI) ions onto activated carbon is an endothermic process, this was for the following reasons:

The importance of temperature in the adsorption of Cr(VI) ions onto activated carbon has been clearly illustrated; hydrogen bonds formed between the solute and solvent at low temperatures can modify the shape and size of the molecules, thus hindering the adsorbate from accessing the micropores of the adsorbent. Such phenomenon was previously observed by Fontecha-Camara et al. (2006), whereby an increase in temperature can result in

Table 6. Thermodynamic parameters for the adsorption of Cr(VI) ions onto “ZRC-AC” at different temperatures.

| Thermodynamic equation : $y = -5629x + 19.05$, $R^2 = 0.999$ | | | |
|---|---------------------------|---------------------------|-----------------------------|
| T (K) | ΔG° (kJ/mol) | ΔH° (kJ/mol) | ΔS° (kJ/mol K) |
| 293 | 0.42 | 46.83 | 199.18 |
| 303 | -1.15 | | |
| 313 | -2.74 | | |

ZRC-AC: *Z. jujuba* rubidium carbonate-activated carbon.

weakening of hydrogen bonds formed between water molecules as well as between water molecules and the solute and/or adsorbent (Terzyk, 2004) which as a result increases the pore diffusion (Costa et al., 1988; García Araya et al., 2003).

This interpretation can be further strengthened by obtaining detailed information about the kind of functional groups present on the surface; those information were obtained following FTIR analyses of our freshly prepared activated carbon (Figure 4(a) and (b)). Figure 5 shows the FTIR spectrum of freshly activated carbon (Figure 4(a)) superimposed on Cr(VI) adsorbed activated carbon (Figure 4(b)). By comparing both spectra, many changes in absorption bands can be mentioned: (i) The decrease in intensity of O–H and/or N–H stretching vibrations ($3446\text{--}3438\text{ cm}^{-1}$) suggests the formation of new interactions between Cr(VI) ions and either the surface O–H and/or NH_2 groups. (ii) The change in intensity as well as the shift in C–H bands ($2922\text{--}2918\text{ cm}^{-1}$) suggests that the adsorption of Cr(VI) ions onto activated carbon has taken effect. (iii) The decrease in C = C absorption intensity between 1624 and 1593 cm^{-1} reflects the presence of interactions between the latter group and Cr(VI) ions. (iv) The drop in intensity of C–O stretching vibrations ($1122\text{--}1042\text{ cm}^{-1}$) implies the participation of C–O groups in the adsorption phenomenon (Hlihor et al., 2015). From these interpretations, we may be able to conclude that O–H, C–O, and C–H groups constitute the main binding sites for Cr(VI) adsorption. Therefore, increasing temperature leads to an increase in the adsorption capacity of Cr(VI); thus, indicating the endothermic nature of the overall adsorption process (positive ΔH°). The positive value of ΔS° suggests the randomness of the adsorption process; as a result, the adsorption phenomenon is entropy driven rather than enthalpy driven. The negative values of ΔG with respect to increasing temperature ($T^\circ\text{C}$) confirm that the adsorption process occurs spontaneously and more favorably. Similar results have been reported by Yang et al. (2015).

Conclusion

In this study, “ZRC-AC,” prepared from *Z. jujuba* cores, a naturally abundant medicinal plant widely used in Algeria for the purpose of food and medicinal treatment was successfully used to remove Cr(VI) from wastewater by adsorption; various kinetic batch experiments were performed to identify the nature of adsorption. The following characteristics were found:

- “ZRC-AC” has a medium surface area, basic pH_{pzc} , and a superior adsorption capacity when compared to other adsorbents cited in literature; such finding is associated with the presence of large micropores on the surface of our activated carbon.

- The adsorption of Cr(VI) by “ZRC-AC” was found to be favorable at pH=2, while the removal efficiency has a proportional relationship with “ZRC-AC” dose; this is unlike other adsorbents whereby the adsorption capacity decreases with an increase in the adsorbent dose.
- The modeling of kinetic data showed that our adsorption experimental data were in good agreement with a pseudo-second-order model.
- The better fit obtained with Langmuir isotherm model suggests that the adsorption of Cr(VI) ions onto activated carbon is homogeneous and of monolayer nature; this model appears to provide the best correlation of experimental data for the adsorption of Cr(VI) than the Freundlich isotherm. The highest monolayer adsorption capacity obtained was 196.38 mg/g.
- The thermodynamic parameters $\Delta H^\circ = 46.83$ kJ/mol, $\Delta S^\circ = 158.49$ J/mol K, and $\Delta G^\circ < 0$ indicate that the adsorption of Cr(VI) ions onto “ZRC-AC” is endothermic, spontaneous, and follows a chemisorption process.

Acknowledgements

We are grateful to Prof. Hamdi Maamar (University of USTHB) for his pertinent critical reviews of the manuscript and English editorial assistance.

Declaration of Conflicting Interests

The author(s) declared no potential conflicts of interest with respect to the research, authorship, and/or publication of this article.

Funding

The author(s) disclosed receipt of the following financial support for the research, authorship, and/or publication of this article: This work was supported by Scientific and Technical Research Center in Physico-chemical Analysis (CRAPC).

References

- Acharya J, Sahu JN, Sahoo BK, et al. (2009) Removal of chromium(VI) from wastewater by activated carbon developed from *Tamarind wood* activated with zinc chloride. *Chemical Engineering Journal* 150: 25–39.
- Alshehri SM, Naushad M, Ahamad T, et al. (2014) Synthesis, characterization of curcumin based ecofriendly antimicrobial bio-adsorbent for the removal of phenol from aqueous medium. *Chemical Engineering Journal* 254: 181–189.
- Anandkumar J and Mandal B (2009) Removal of Cr(VI) from aqueous solution using Bael fruit (*Aegle marmelos correa*) shell as an adsorbent. *Journal of Hazardous Materials* 168: 633–640.
- Babel S and Kurniawan TA (2004) Cr(VI) removal from synthetic wastewater using coconut shell charcoal and commercial activated carbon modified with oxidizing agents and/or chitosan. *Chemosphere* 54: 951–967.
- Baral A and Engelken RD (2002) Chromium based regulations and greening in metal finishing industries in the USA. *Environmental Science & Policy* 5: 121–133.
- Barrera-Diaz CE, Lugo-Lugo V and Bilyeu B (2012) A review of chemical, electrochemical and biological methods for aqueous Cr(VI) reduction. *Journal of Hazardous Materials* 223–224: 1–12.
- Bayramoglou G, Celik G, Yalcin E, et al. (2005) Modification of surface properties of *Lentinus sajor-caju* mycelia by physical and chemical methods: Evaluation of their Cr⁺⁶ removal efficiencies from aqueous medium. *Journal of Hazardous Materials* 119: 219–229.

- Benturki O. (2008) Thèse de doctorat d'état de l'université des sciences et de la technologie, USTHB, Algeria, p.230.
- Bishnoi NR, Bajaj M, Sharma N, et al. (2004) Adsorption of Cr(VI) on activated rice husk carbon and activated alumina. *Bioresource Technology* 91: 305–307.
- Bouras HD, Benturki O, Bouras N, et al. (2015) The use of an agricultural waste material from *Ziziphus jujuba* as a novel adsorbent for humic acid removal from aqueous solutions. *Journal of Molecular Liquids* 211: 1039–1046.
- Burg P, Fydrych P, Cagniant D, et al. (2002) The characterization of nitrogen-enriched activated carbons by IR, XPS and LSER methods. *Carbon* 40: 1521–1531.
- Ciopec M, Davidescu CM, Negrea A, et al. (2012) Adsorption studies of Cr (III) ions from aqueous solutions by DEHPA impregnated onto Amberlite XAD7- Factorial design analysis *Chemical Engineering Research and Design* 90: 1660. Adsorption studies of Cr (III) ions from aqueous solutions by DEHPA impregnated onto Amberlite XAD7- Factorial design analysis
- Costa E, Calleja G, Marijua, et al. (1988) Comparative adsorption of phenol, p-nitrophenol and p-hydroxybenzoic acid on activated carbon. *Adsorption Science & Technology* 5: 213–228.
- Cronje KJ, Chetty K, Carsky M, et al. (2011) Optimization of chromium(VI) sorption potential using developed activated carbon from sugarcane bagasse with chemical activation by zinc chloride. *Desalination* 275: 276–284.
- Dakiky M, Khamis M, Manassra A, et al. (2002) Selective adsorption of chromium(VI) in industrial wastewater using low-cost abundantly available adsorbents. *Advances in Environmental Research* 6: 533–540.
- Demiral H, Demiral I, Tumsek F, et al. (2008) Adsorption of chromium(VI) from aqueous solution by activated carbon derived from olive bagasse and applicability of different adsorption models. *Chemical Engineering Journal* 144: 188–196.
- Demirbas E, Kobya M, Senturk E, et al. (2004) Adsorption kinetics for the removal of chromium(VI) from aqueous solutions on the activated carbons prepared from agricultural wastes. *Water SA* 30: 533–539.
- Deveci H and Kar Y (2013) Adsorption of hexavalent chromium from aqueous solutions by bio-chars obtained during biomass pyrolysis. *Journal of Industrial and Engineering Chemistry* 19: 190–196.
- Dobrowolski R and Stefaniak E (2000) Study of chromium(VI) adsorption from aqueous solution on to activated carbon. *Adsorption Science & Technology* 18: 97–106.
- Donmez G and Aksu Z (2002) Removal of chromium(VI) from saline wastewaters by *Dunaliella* species. *Process Biochemistry* 38: 751–762.
- Driel J, Capelle A and De Vooy F (1983) *Activated Carbon a Fascination Material*. Amersfoort: Norit, p.40.
- Dubey SP and Gopal K (2007) Adsorption of chromium(VI) on low cost adsorbents derived from agricultural waste material: A comparative study. *Journal of Hazardous Materials* 145: 465–470.
- Duranoglu D, Trochimczuk AW and Beker U (2010) A comparison study of peach stone and acrylonitrile-divinylbenzene copolymer based activated carbons as chromium(VI) sorbents. *Chemical Engineering Journal* 165: 56–63.
- El-Shafey EI (2005) Behavior of reduction-sorption of chromium(VI) from an aqueous solution on a modified rice husk. *Water, Air, and Soil Pollution* 163: 81–102.
- Fontecha-Camara MA, Lopez-Ramon MV, Alvarez-Merino MA, et al. (2006) About the endothermic nature of the adsorption of the herbicide diuron from aqueous solutions on activated carbon fiber. *Carbon* 44: 2330–2356.
- García Araya JF, Beltrán FJ, Álvarez P, et al. (2003) Activated carbon adsorption of some phenolic compounds present in agroindustrial wastewater. *Adsorption* 9: 107–115.
- Garg UK, Kaur MP, Garg VK, et al. (2007) Removal of hexavalent chromium from gaseous solution by agricultural waste biomass. *Journal of Hazardous Materials* 140: 60–68.
- Ghosh PK (2009) Hexavalent chromium Cr(VI) removal by acid modified waste activated carbons. *Journal of Hazardous Materials* 171: 116–122.

- Glireas FW, Tarars MJ and Ingols RS (1965) *Standard Methods for the Examination of Water and Wastewater*. 12th ed. New York: American Public Health Association (APHA) Inc, p.213.
- Giri AK, Patel R and Mandal S (2012) Removal of Cr(VI) from aqueous solution by *Eichhornia crassipes* root biomass-derived activated carbon. *Chemical Engineering Journal* 185–186: 71–81.
- Gottipati R and Mishra S (2010) Process optimization of adsorption of Cr(VI) on activated carbons prepared from plant precursors by a two-level full factorial design. *Chemical Engineering Journal* 160: 99–107.
- Gregg SJ and Sing KSW (1982) *Adsorption, Surface Area and Porosity*. London: Academic Press, p.100.
- Gueye M, Richardson Y, Kafack FT, et al. (2014) High efficiency activated carbons from African biomass residues for the removal of chromium(VI) from wastewater. *Journal of Environmental Chemical Engineering* 2: 273–281.
- Hafez AI, El-Manharawy MS and Khedr MA (2002) RO membrane removal of unreacted chromium from spent tanning effluent. A pilot-scale study, Part 2. *Desalination* 144: 237–242.
- Hall KR, Eagleton LC, Acrivos A, et al. (1966) Pore and solid diffusion kinetics in fixed-bed adsorption under constant pattern conditions. *Industrial & Engineering Chemistry Fundamentals* 5: 212–223.
- Hamadi NK, Chen XD, Farid MM, et al. (2001) Adsorption kinetics for the removal of chromium(VI) from aqueous solution by adsorbents derived from used tyres and sawdust. *Chemical Engineering Journal* 84: 95–105.
- Hamdaoui W and Naffrechoux E (2007) Modeling of adsorption isotherms of phenol and chlorophenols onto granular activated carbon Part II. Models with more than two parameters. *Journal of Hazardous Materials* 147: 401–411.
- Hlihor RM, Diaconu M, Leon F, et al. (2015) Experimental analysis and mathematical prediction of Cd (II) removal by biosorption using support vector machines and genetic algorithms. *New Biotechnology* 32: 358–368.
- Ho YS and McKay G (1999) Pseudo-second-order model for sorption processes. *Process Biochemistry* 34: 451–465.
- Hsu N, Wang S, Liao Y, et al. (2009) Removal of hexavalent chromium from acidic aqueous solutions using rice straw-derived carbon. *Journal of Hazardous Materials* 171: 1066–1070.
- Jain M, Garg VK and Kadirvelu K (2009) Chromium(VI) removal from aqueous system using *Helianthus annuus* (sunflower) stem waste. *Journal of Hazardous Materials* 162: 365–372.
- Kadirvelu K and Namasivayam C (2003) Activated carbon from coconut coir pith as metal adsorbent: Adsorption of Cd (II) from aqueous solution. *Advances in Environmental Research* 7: 471–478.
- Karthikeyan T, Rajgopal S and Miranda LR (2005) Chromium(VI) adsorption from aqueous solution by *Hevea brasiliensis* sawdust activated carbon. *Journal of Hazardous Materials* B124: 192–199.
- Kennedy LJ, Judith Vijaya J, Kayalvizhi K, et al. (2007) Adsorption of phenol from aqueous solutions using mesoporous carbon prepared by two-stage process. *Chemical Engineering Journal* 132: 279–287.
- Khan AR, Ataullah A and Al-Haddad A (1997) Equilibrium adsorption studies of some aromatic pollutants from dilute aqueous solutions on activated carbon at different temperatures. *Journal of Colloid and Interface Science* 194: 154–165.
- Khezami L and Capart R (2005) Removal of chromium(VI) from aqueous solution by activated carbons: Kinetic and equilibrium studies. *Journal of Hazardous Materials* B123: 223–231.
- Kiran B, Kaushik A and Kaushik CP (2007) Response surface methodological approach for optimizing removal of Cr(VI) from aqueous solution using immobilized cyanobacterium. *Chemical Engineering Journal* 126: 147–153.
- Kobya M (2004) Removal of Cr(VI) from aqueous solutions by adsorption onto hazelnut shell activated carbon: Kinetic and equilibrium studies. *Bioresource Technology* 91: 317–321.
- Lagergren S (1898) Zur theorie der sogenannten adsorption gelöster stoffe, Kungliga Svenska Vetenskapsakad. *Handling* 24: 1–35.

- Lima LSD, Araujo MDM, Quinaia SP, et al. (2011) Adsorption modeling of Cr, Cd and Cu on activated carbon of different origins by using fractional factorial design. *Chemical Engineering Journal* 166: 881–889.
- Liu CC, Wang MK, Chiou CS, et al. (2006) Chromium removal and sorption mechanism from aqueous solutions by wine processing waste sludge. *Industrial & Engineering Chemistry Research* 45: 8891–8899.
- Liu H, Liang S, Gao J, et al. (2014) Enhancement of Cr(VI) removal by modifying activated carbon developed from *Zizania caduciflora* with tartaric acid during phosphoric acid activation. *Chemical Engineering Journal* 24: 168–174.
- Liu W, Zhang J, Zhang C, et al. (2010) Adsorptive removal of Cr(VI) by Fe-modified activated carbon prepared from *Trapa natans* husk. *Chemical Engineering Journal* 162: 677–684.
- Lopez-Ramon MV, Stoeckli F, Moreno-Castilla C, et al. (1999) On the characterization of acidic and basic surface sites on carbons by various techniques. *Carbon* 37: 1215–1221.
- Malkoç E, Nuhoglu Y and Dundar M (2006) Adsorption of chromium(VI) on pomace – An olive oil industry waste: Batch and column studies. *Journal of Hazardous Materials B* 138: 142–151.
- Meena AK, Kadirvelu K, Mishra GK, et al. (2008) Adsorptive removal of heavy metals from aqueous solution by treated sawdust (*Acacia arabica*). *Journal of Hazardous Materials* 150: 604–611.
- Mohanty K, Jha M, Meikap BC, et al. (2005) Removal of chromium(VI) from dilute aqueous solutions by activated carbon developed from *Terminalia arjuna* nuts activated with zinc chloride. *Chemical Engineering Science* 60: 3049–3059.
- Mohanty K, Jha M, Meikap BC, et al. (2006) Biosorption of Cr(VI) from aqueous solution by *Eichhornia crassipes*. *Chemical Engineering Journal* 117: 71–77.
- Monser L and Adhoum N (2002) Modified activated carbon for the removal of copper, zinc, chromium and cyanide from wastewater. *Separation and Purification Technology* 26: 137–146.
- Mullah AH and Robinson CW (1996) Pentachlorophenol adsorption and desorption characteristics of granular activated carbon – I. Isotherms. *Water Research* 30: 2901–2906.
- Nabi SA, Bushra R, Al-Othman ZA, et al. (2011) Synthesis, characterization and analytical applications of a new composite cation exchange material acetonitrile stannic (IV) selenite: Adsorption behavior of toxic metal ions in nonionic surfactant medium. *Separation Science and Technology* 46: 847–857.
- Naushad M (2014) Surfactant assisted nano-composite cation exchanger: Development, characterization and applications for the removal of toxic Pb^{2+} from aqueous medium. *Chemical Engineering Journal* 235: 100–108.
- Nemr AE, Khaled A, Abdelwahab O, et al. (2008) Treatment of wastewater containing toxic chromium using new activated carbon developed from date palm seed. *Journal of Hazardous Materials* 152: 263–275.
- Oliveira EA, Montanher SF, Andrade AD, et al. (2005) Equilibrium studies for the adsorption of chromium and nickel from aqueous solutions using raw rice bran. *Process Biochemistry* 40: 3485–3490.
- Ozkaya B (2006) Adsorption and desorption of phenol on activated carbon and a comparison of isotherm models. *Journal of Hazardous Materials* 129: 158–163.
- Pandey PK, Sharma SK and Sambi SS (2010) Kinetic and equilibrium study of chromium adsorption on zeolite NaX. *International Journal of Environmental Science & Technology* 7 (2): 395–404.
- Park D, Yun YS, Kim JY, et al. (2008) How to study Cr(VI) biosorption: Use of fermentation waste for detoxifying Cr(VI) in aqueous solution. *Chemical Engineering Journal* 136: 173–179.
- Ranganathan K (2000) Chromium removal by activated carbons prepared from *Casurina equisetifolia* leaves. *Bioresource Technology* 73: 99–103.
- Rao M, Parwate AV and Bhole AG (2002) Removal of Cr^{6+} and Ni^{2+} from aqueous solution using bagasse and fly ash. *Waste Management* 22: 821–830.
- Rao MM, Rao GP, Seshaiiah K, et al. (2008) Activated carbon from *Ceiba pentandra* hulls, an agricultural waste, as an adsorbent in the removal of lead and zinc from aqueous solutions. *Waste Management* 28: 849–858.

- Sahinkaya E, Altun M, Bektas S, et al. (2012) Bioreduction of Cr(VI) from acidic wastewaters in a sulfidogenic ABR. *Minerals Engineering* 32: 38–44.
- Sedlak DL and Chan PG (1997) Reduction of hexavalent chromium by ferrous iron. *Geochimica et Cosmochimica Acta* 61: 2185–2192.
- Sekaran G, Karthikeyan S, Gupta VK, et al. (2013) Immobilization of *Bacillus* sp. in mesoporous activated carbon for degradation of sulphonated phenolic compound in wastewater. *Materials Science & Engineering C, Materials for Biological Applications* 33: 735–745.
- Selvi K, Pattabhi S and Kadirvelu K (2001) Removal of Cr(VI) from aqueous solution by adsorption onto activated carbon. *Bioresource Technology* 80: 87–89.
- Sing KSW, Everett DH, Haul RAW, et al. (1985) Reporting physiosorption data for gas/solid systems with special surface area and porosity. *Pure and Applied Chemistry* 57: 603–619.
- Sips R (1948) On the structure of a catalyst surface. *Journal of Chemical Physics* 16: 490–495.
- Smith JM (1981) *Chemical Engineering Kinetic*. 3rd ed. Singapore: McGraw-Hill.
- Suksabye P and Thiravetyan P (2012) Cr(VI) adsorption from electroplating plating wastewater by chemically modified coir pith. *Journal of Environmental Management* 102: 1–8.
- Temkin MI (1941) Adsorption equilibrium and the kinetics of processes on non homogeneous surfaces and in the interaction between adsorbed molecules. *Zhurnal fizicheskoi khimii* 15: 296–332.15
- Terzyk AP (2004) Molecular properties and intermolecular forces-factors balancing the effect of carbon surface chemistry in adsorption of organics from dilute aqueous solutions. *Journal of Colloid and Interface Science* 275: 9–29.
- Tiravanti G, Petruzzelli D and Passiono R (1997) Pretreatment of tannery wastewaters by an ion exchange process for Cr(III) removal and recovery. *Water Science and Technology* 36: 197–207.
- Tóth J (2000) Calculation of the BET-compatible surface area from any type I isotherms measured above the critical temperature. *Journal of Colloid and Interface Science* 225: 378–383.
- Tseng RL and Tseng SK (2006) Characterization and use of high surface area activated carbons prepared from cane pith for liquid-phase adsorption. *Journal of Hazardous Materials B136*: 671–680.
- Ucum H, Bayham YK, Kay Y, et al. (2002) Biosorption of chromium(VI) from aqueous solution by cone biomass of *Pinus sylvestris*. *Bioresource Technology* 85: 155–158.
- Verma A, Chakraborty S and Basu JK (2006) Adsorption study of hexavalent chromium using tamarind hull-based adsorbents. *Separation and Purification Technology* 50: 336–341.
- Vijayaraghavan K, Padmesh TVN, Palanivelu K, et al. (2006) Biosorption of nickel(II) ions onto *Sargassum wightii*: Application of two-parameter and three-parameter isotherm models. *Journal of Hazardous Materials* 133: 304–308.
- Wang JL and Chen C (2006) Biosorption of heavy metals by *Saccharomyces cerevisiae*: A review. *Biotechnology Advances* 24: 427–451.
- Wang L, Xing R, Liu S, et al. (2010) Studies on adsorption behavior of Pb (II) onto a thiourea-modified chitosan resin with Pb (II) as template. *Carbohydrate Polymers* 81: 305–310.
- Wu Y, Li B, Feng S, et al. (2009) Adsorption of Cr(VI) and As (III) on coaly activated carbon in single and binary systems. *Desalination* 249: 1067–1073.
- Yang J, Yu M and Chen W (2015) Adsorption of hexavalent chromium from aqueous solution by activated carbon prepared from Longan seed: Kinetics, equilibrium and thermodynamics. *Journal of Industrial and Engineering Chemistry* 21: 414–422.
- Yang J, Yu M and Qiu T (2014) Adsorption thermodynamics and kinetics of Cr(VI) on KIP210 resin. *Journal of Industrial and Engineering Chemistry* 20: 480–486.
- Zhang H, Tang Y, Cai D, et al. (2010) Hexavalent chromium removal from aqueous solution by algal bloom residue derived activated carbon: Equilibrium and kinetic studies. *Journal of Hazardous Materials* 181: 801–808.
- Zielke U, Huttinger KJ and Hoffman WP (1996) Surface oxidized carbon fibers: I. Surface structure and chemistry. *Carbon* 34: 983–998.